Journal of Scientific Computing (2019) 81:1767–1800
https://doi.org/10.1007/s10915-019-01062-6

Numerical Schemes for Solving the Time-Fractional Dual-Phase-Lagging Heat Conduction Model in a Double-Layered Nanoscale Thin Film

Cui-cui Ji[1] · Weizhong Dai[2] · Zhi-zhong Sun[3]

Received: 8 April 2019 / Revised: 20 September 2019 / Accepted: 30 September 2019 /
Published online: 9 October 2019

Abstract
This article proposes a time fractional dual-phase-lagging (DPL) heat conduction model in a double-layered nanoscale thin film with the temperature-jump boundary condition and a thermal lagging effect interfacial condition between layers. The model is proved to be well-posed. A finite difference scheme with second-order spatial convergence accuracy in maximum norm is then presented for solving the fractional DPL model. Unconditional stability and convergence of the scheme are proved by using the discrete energy method. A numerical example without exact solution is given to verify the accuracy of the scheme. Finally, we show the applicability of the time fractional DPL model by predicting the temperature rise in a double-layered nanoscale thin film, where a gold layer is on a chromium padding layer exposed to an ultrashort-pulsed laser heating.

Keywords Nanoscale heat transfer · Fractional dual-phase-lagging model · Temperature-jump boundary condition · Interfacial condition · Finite difference scheme · Stability · Convergence

Cui-cui Ji and Zhi-zhong Sun were supported by National Natural Science Foundation of China (No. 11671081).

✉ Zhi-zhong Sun
zzsun@seu.edu.cn

Cui-cui Ji
cuicuiahuan@163.com

Weizhong Dai
dai@coes.latech.edu

[1] School of Mathematics and Statistics, Qingdao University, Qingdao 266071, People's Republic of China

[2] Mathematics and Statistics, Louisiana Tech University, Ruston, LA 71272, USA

[3] School of Mathematics, Southeast University, Nanjing 210096, People's Republic of China

1 Introduction

When dealing with micro/nano scale heat conduction, such as thin film exposed to ultrashort-pulsed laser heating or thermal analysis in nanoscale metal-oxide-semiconductor field-effect-transistor (MOSFET) in the semiconductor industry, the dual-phase-lagging (DPL) model,

$$\rho c_\rho (T_t + \tau_q T_{tt})(x,t) = \kappa (T + \tau_T T_t)_{xx}(x,t) + f(x,t), \tag{1}$$

is one of excellent candidates for solving micro/nanoscale heat transfer problems [1–9]. The DPL model was derived based on the non-Fourier's law

$$q(x,t) + \tau_q q_t(x,t) = -\kappa (T + \tau_T T_t)_x(x,t), \tag{2}$$

coupled with the energy equation

$$\rho c_\rho T_t(x,t) = -q_x(x,t) + S(x,t). \tag{3}$$

Here, κ is the conductivity, τ_q, τ_T are the phase lags of the heat flux q and temperature gradient ∇T, respectively, ρ and c_ρ denote the density and the specific heat of the material, respectively, and $f(x,t) = S(x,t) + \tau_q S_t(x,t)$, where $S(x,t)$ is a source term.

Fractional calculus has been successfully used to modulate several models in heat conduction and other media and has gained importance in heat conduction and thermoelastic problems [10]. Sherief et al. [11] have proposed the fractional non-Fourier law as $q + \tau_q {}_0^C D_t^\alpha q = -\kappa T_x$, $0 < \alpha < 1$, where ${}_0^C D_t^\alpha$ is the Caputo-type time-fractional derivative such that ${}_0^C D_t^\alpha u(t) = \frac{1}{\Gamma(1-\alpha)} \int_0^t \frac{u'(s)}{(t-s)^\alpha} ds$, $0 < \alpha < 1$, $\Gamma(\cdot)$ is the gamma function [12]. Results show a good agreement with experimental data when using fractional derivatives for description of viscoelastic materials [11]. Youssef [13] has assumed another form for the nonlocal non-Fourier law as $q + \tau_q q_t = -\kappa I^{\alpha-1} T_x$, $0 < \alpha \le 2$, where I^α is the Riemann-Louisville fractional integral such that $I^\alpha u(t) = \frac{1}{\Gamma(n-\alpha)} \frac{d^n}{dt^n} \int_0^t \frac{u(s)}{(t-s)^{\alpha-n+1}} ds$, $n-1 \le \alpha < n$, as given in [14]. When $\alpha > 1$, it indicates the strong conductivity [14]. Yu et al. [15] has applied the fractional-order generalized DPL model for nanoscale heat transfer in electro-magneto-thermoelastic media. It has been reported that there is larger heat conductivity for nanostructured carbon materials [16,17]. Thus, the fractional-order generalized DPL model that includes the concept of non-locality [18] can be an excellent candidate for such a nanoscale heat transfer. Recently, we [19] have studied a time-fractional DPL heat conduction equation

$$\rho c_\rho \left(T_t + \frac{(\tau_q)^\alpha}{\Gamma(1+\alpha)} {}_0^C D_t^{\alpha+1} T \right)(x,t) = \kappa \left(T + \frac{(\tau_T)^\alpha}{\Gamma(1+\alpha)} \cdot {}_0^C D_t^\alpha T \right)_{xx}(x,t) + f(x,t). \tag{4}$$

Here, $\kappa = \rho c_\rho |v| \frac{\ell_f}{3}$ where ℓ_f is the phonon mean free path, $|v|$ is the heat carrier group velocity and $|v| = \frac{\ell_f}{\tau_q}$, $f(x,t) = S(x,t) + \frac{(\tau_q)^\alpha}{\Gamma(1+\alpha)} {}_0^C D_t^\alpha S(x,t)$ and the Caputo fractional derivatives [20] are defined by

$$ {}_0^C D_t^\alpha T(x,t) = \frac{1}{\Gamma(1-\alpha)} \int_0^t \frac{T_s(x,s)}{(t-s)^\alpha} ds, \quad t > 0, \quad 0 < \alpha < 1,$$

$$ {}_0^C D_t^{\alpha+1} T(x,t) = \frac{1}{\Gamma(1-\alpha)} \int_0^t \frac{T_{ss}(x,s)}{(t-s)^\alpha} ds, \quad t > 0, \quad 0 < \alpha < 1.$$

We chose the Caputo fractional definition for two reasons. One is that the Caputo derivative allows the utilization of physically interpretable initial conditions [20]. The other is that $L1$ approximation for the Caputo derivative is well-developed, which we will use for the development of the numerical scheme in this study.

By introducing these non-dimensional parameters:

$$u = \frac{T - T_0}{T_0}, \quad t_\star = [\Gamma(1+\alpha)]^{\frac{1}{\alpha}} \frac{t}{\tau_q}, \quad x_\star = \frac{x}{L_c}, \quad K_n = \frac{\ell_f}{L_c}, \quad B = \frac{\tau_T}{\tau_q},$$

where L_c is the characteristic length, and K_n is the Knudsen number, we obtained a fractional DPL model in dimensionless form as follows (without asterisk):

$$u_t(x,t) + {}_0^C D_t^{\alpha+1} u(x,t) = \frac{K_n^2}{3[\Gamma(1+\alpha)]^{1/\alpha}} \left(u + B^\alpha \cdot {}_0^C D_t^\alpha u \right)_{xx} (x,t) + F(x,t) \quad (5)$$

with the temperature-jump boundary conditions

$$-\gamma K_n u_x(0,t) + u(0,t) = \phi_1(t), \quad \gamma K_n u_x(L,t) + u(L,t) = \phi_2(t), \quad (6)$$

and the initial condition

$$u(x,0) = \varphi(x), \quad u_t(x,0) = \psi(x). \quad (7)$$

In [19], we further proposed an accurate and unconditionally stable finite difference scheme for solving the above fractional DPL model. By changing K_n and fractional order α, we applied the fractional DPL model to simulate a simple nanoscale semiconductor silicon device. Results indicate that our model can be an excellent candidate for analyzing the temperature instability appearing in electronic [21].

It is noted that layered structures have appeared in many engineering systems such as biological tissues, micro-electronic devices, thin films, reactor walls, thermoelectric power conversion, thermal coating, metal oxide semiconductors, and thermal processing of DNA origami nanostructures [4,22–25]. In particular, the multi-layered metal thin-films, for example, gold-coated metal mirrors, are often used in high-power infrared-laser systems to avoid thermal damage at the front surface of a single layer film caused by the high-power laser energy [26]. Furthermore, to achieve high thermoelectric efficiency, a low thermal conductivity is required. Low thermal conductivity is often realized by nano-structuring with the introduction of a high density of materials [24]. All semiconductor devices possess metal contacts and hence the study of heat transport through metal-semiconductor interfaces is a technologically relevant problem [27]. Thus, analyzing heat transfer in layered structures is of crucial importance for the design and operation of nano-devices and the optimization of thermal processing of nano-materials.

For this purpose, we extend our study to the multilayered structure case and propose a time fractional DPL heat conduction model in a double-layered nanoscale thin film, as shown in Fig. 1. We then develop a second-order finite difference scheme for solving the fractional DPL model. The rest of the article is organized as follows: In Sect. 2, we propose a fractional DPL heat conduction model for nanoscale heat conduction in a double-layered thin film with the temperature-jump boundary condition and a thermal lagging effect interfacial condition between layers. In Sect. 3, we obtain an energy estimate for ensuring the mathematical model to be well-posed. Some useful notations and lemmas are presented in Sect. 4. After that, we construct a finite difference scheme for solving the mathematical model. In Sect. 5, the unconditional stability and convergence of the scheme are rigorously analyzed. In Sect. 6, we provide a numerical example to support the theoretical analysis and then apply the numerical

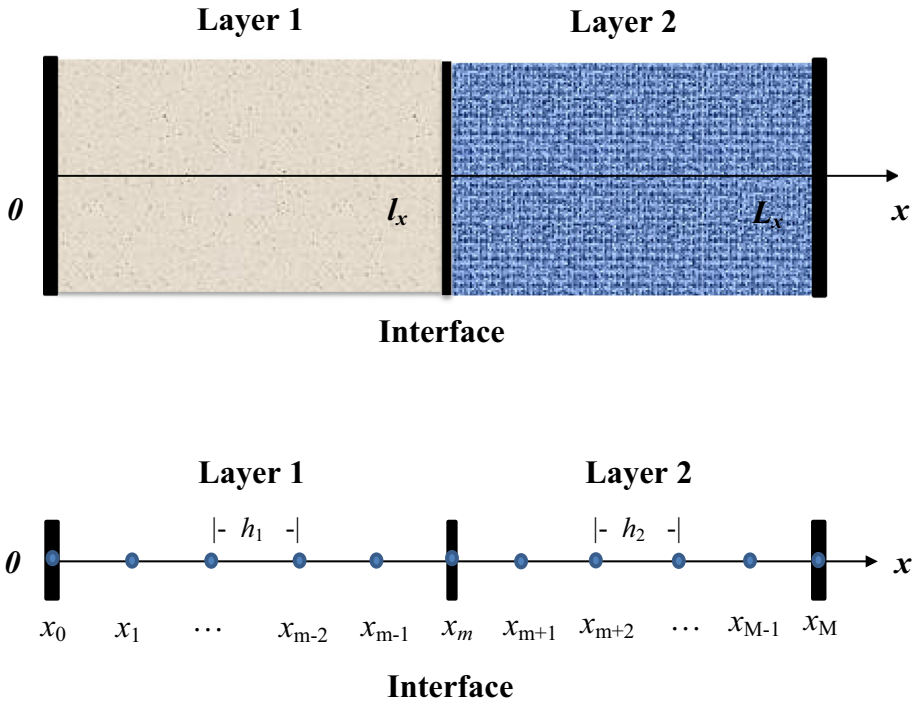

Fig. 1 Double-layered structure (above) and the mesh for numerical schemes (below)

scheme to the thermal analysis for a gold thin layer on a chromium padding layer irradiated by an ultrashort-pulsed laser. Finally, we summarize the major results of this work in Sect. 7.

2 Time Fractional DPL Heat Conduction Model

Consider the time fractional DPL heat conduction equations in a double-layered nanoscale thin film as follows:

$$\rho_1 c_\rho^1 \left(T_t + \frac{(\tau_{q,1})^\alpha}{\Gamma(1+\alpha)} {}_0^C D_t^{\alpha+1} T \right)(x,t) = \kappa_1 \left(T + \frac{(\tau_{T,1})^\beta}{\Gamma(1+\beta)} {}_0^C D_t^\beta T \right)_{xx}(x,t) + f_1(x,t), \quad x \in (0, l_x'), \ t \in (0, L_t'], \tag{8}$$

$$\rho_2 c_\rho^2 \left(T_t + \frac{(\tau_{q,2})^\alpha}{\Gamma(1+\alpha)} {}_0^C D_t^{\alpha+1} T \right)(x,t) = \kappa_2 \left(T + \frac{(\tau_{T,2})^\beta}{\Gamma(1+\beta)} {}_0^C D_t^\beta T \right)_{xx}(x,t) + f_2(x,t), \quad x \in (l_x', L_x'), \ t \in (0, L_t'], \tag{9}$$

where $0 < \alpha, \beta < 1$. Introducing several non-dimensional parameters:

$$u = \frac{T - T_0}{T_0}, \quad t_\star = \frac{t}{\tau_{q,1} + \tau_{q,2}}, \quad x_\star = \frac{x}{L_c}, \quad K_{\mathrm{n},i} = \frac{\ell_{f,i}}{L_c}, \quad B_i = \frac{\tau_{T,i}}{\tau_{q,1} + \tau_{q,2}}, \quad i = 1, 2$$

where $\ell_{f,i}$ and L_c are the phonon free path length and the characteristic length in different layer nanoscale thin films, respectively.

Let $\eta_1 = \frac{\tau_{q,1}}{\tau_{q,1}+\tau_{q,2}}$ and $\eta_2 = \frac{\tau_{q,2}}{\tau_{q,1}+\tau_{q,2}}$. We can express the governing equations (8) and (9) in a dimensionless form by omitting the subscripts of the non-dimensional parameters $x_\star$ and $t_\star$ as follows,

$$u_t(x,t) + \frac{\eta_1^\alpha}{\Gamma(1+\alpha)} {}_0^C D_t^{\alpha+1} u(x,t) = \frac{K_{\mathrm{n},1}^2}{3\eta_1}\left(u + \frac{B_1^\beta}{\Gamma(1+\beta)} {}_0^C D_t^\beta u\right)_{xx}(x,t) + F_1(x,t),\ x \in (0,l_x),\ t \in (0,L_t], \tag{10}$$

$$u_t(x,t) + \frac{\eta_2^\alpha}{\Gamma(1+\alpha)} {}_0^C D_t^{\alpha+1} u(x,t) = \frac{K_{\mathrm{n},2}^2}{3\eta_2}\left(u + \frac{B_2^\beta}{\Gamma(1+\beta)} {}_0^C D_t^\beta u\right)_{xx}(x,t) + F_2(x,t),\ x \in (l_x,L_x),\ t \in (0,L_t], \tag{11}$$

with the source terms

$$F_1(x,t) = \frac{\tau_{q,1}+\tau_{q,2}}{\rho_1 c_1 T_0} f_1(x,t), \quad x \in (0,l_x), \quad t \in (0,L_t],$$
$$F_2(x,t) = \frac{\tau_{q,1}+\tau_{q,2}}{\rho_2 c_2 T_0} f_2(x,t), \quad x \in (l_x,L_x), \quad t \in (0,L_t].$$

Based on the assumption of the perfect thermal contact between double layers, we propose the interfacial conditions at $x = l_x$ below

$$u(l_x-0,t) = u(l_x+0,t), \quad t \in [0,L_t], \tag{12}$$

$$\frac{K_{\mathrm{n},1}^2}{\eta_1}\left(u + \frac{B_1^\beta}{\Gamma(1+\beta)} {}_0^C D_t^\beta u\right)_x (l_x-0,t) = \frac{K_{\mathrm{n},2}^2}{\eta_2}\left(u + \frac{B_2^\beta}{\Gamma(1+\beta)} {}_0^C D_t^\beta u\right)_x (l_x+0,t), \quad t \in [0,L_t], \tag{13}$$

which ensures that the normalized fractional DPL model is well-posed. In order to catch the effects of boundary phonon scattering inside a nano-size geometry, the temperature-jump boundary conditions [19,28] are introduced as follows,

$$-\gamma_1 K_{\mathrm{n},1} u_x(0,t) + u(0,t) = \phi_1(t), \quad t \in (0,L_t], \tag{14}$$
$$\gamma_2 K_{\mathrm{n},2} u_x(L_x,t) + u(L_x,t) = \phi_2(t), \quad t \in (0,L_t], \tag{15}$$

together with the initial conditions

$$u(x,0) = \varphi(x), \quad u_t(x,0) = \psi(x), \quad x \in [0,L_x]. \tag{16}$$

It should be pointed out that from Eqs. (8) to (9), we can see that when $\alpha = \beta = 0$, the fractional DPL heat conduction equation reduces to the traditional heat conduction equation, and on the other hand, when $\alpha = \beta = 1$, it reduces to the DPL heat conduction equation with integer order derivatives. To see how the temperature changes from the traditional heat conduction equation to the DPL heat conduction equation with integer order derivatives, we consider only the case when $0 \le \alpha, \beta \le 1$. This may be considered as some type of sub-DPL heat conduction behavior.

3 Well Posedness of the Fractional DPL Model

In our recent work [19], an energy estimation for the time fractional DPL in a single nanoscale thin film with the fractional order $\alpha = \beta$, i.e.,

$$u_t(x,t) + \frac{\eta^\alpha}{\Gamma(1+\alpha)} {}_0^C D_t^{\alpha+1} u(x,t) = \frac{K_n^2}{3\eta}\left(u + \frac{B^\alpha}{\Gamma(1+\alpha)} {}_0^C D_t^\alpha u\right)_{xx}(x,t) + F(x,t), \quad x \in (0, L_x), \quad t \in (0, L_t], \tag{17}$$

was deduced by introducing an intermediate variable

$$v(x,t) = u(x,t) + \frac{B^\alpha}{\Gamma(1+\alpha)} \cdot {}_0^C D_t^\alpha u(x,t). \tag{18}$$

This transform brings in an inevitable restriction on the initial condition $u_t(x,0) = 0$ when exchanging the first-order differential operator D_t and the Caputo fractional operator ${}_0^C D_t^\alpha$. The commutativity of the two operators is needed in the proof of Theorem 2.3 in [19]. To detour this restrictive condition, in this section, we do not introduce an intermediate variable like (18), but flexibly utilize the corresponding properties of the Caputo fractional derivative ${}_0^C D_t^\alpha$ $(0 < \alpha < 1)$ to verify that the time fractional DPL system in a double-layered nanoscale thin films (10)–(16) is well-posed. This will ensure that the presented energy function can be effectively controlled by the initial values and the source terms.

We now present several useful lemmas with respect to the Caputo fractional derivative operator ${}_0^C D_t^\alpha$ $(0 < \alpha < 1)$, which will be used for obtaining an energy estimation of the governing model (10)–(16). We firstly introduce the Riemann-Liouville (RL) fractional integral of order α [20],

$${}_0^{RL} D_t^{-\alpha} y(t) = \frac{1}{\Gamma(\alpha)} \int_0^t \frac{y(\xi) d\xi}{(t-\xi)^{1-\alpha}}, \quad t > 0, \quad \alpha > 0, \tag{19}$$

and the RL fractional derivative of order α ,

$${}_0^{RL} D_t^{\alpha} y(t) = \frac{1}{\Gamma(1-\alpha)} \frac{d}{dt} \int_0^t \frac{y(\xi) d\xi}{(t-\xi)^{\alpha}}, \quad t > 0, \quad 0 < \alpha < 1. \tag{20}$$

Lemma 1 *For any function $y(t) \in C^1([0,T])$, if $0 < \alpha < 1$, it holds that*

$$y'(t) \cdot {}_0^C D_t^\alpha y(t) = \frac{1}{2} \frac{d}{dt} {}_0^{RL} D_t^{-\alpha} \left({}_0^C D_t^\alpha y(t)\right)^2 + \frac{1-\alpha}{2\Gamma(\alpha)} \int_0^t \left(\left[\int_0^\xi \frac{\left({}_0^C D_\eta^\alpha y(\eta)\right)'}{(t-\eta)^{1-\alpha}} d\eta \right] \frac{1}{(t-\xi)^\alpha} d\xi \right)^2, \quad t \in (0,T], \quad 0 < \alpha < 1. \tag{21}$$

Proof For simplicity, denote

$$G[y](\alpha, t) = \frac{\alpha}{2\Gamma(1-\alpha)} \int_0^t \frac{d\xi}{(t-\xi)^{1-\alpha}} \left(\int_0^\xi \frac{y_\eta(\eta)}{(t-\eta)^\alpha} d\eta \right)^2.$$

Alikhanov [29] proved that if $0 < \alpha < 1$,

$$y(t) \cdot {}_0^C D_t^\alpha y(t) = \frac{1}{2} {}_0^C D_t^\alpha y^2(t) + G[y](\alpha, t). \tag{22}$$

We further notice the fact ${}_0^C D_t^\alpha y(t)|_{t=0} = 0$ and use the relation (22). The detailed process is shown as follows,

$$
\begin{aligned}
y'(t)\cdot {}_0^C D_t^{\alpha} y(t) &= {}_0^{RL} D_t^{1-\alpha}\left({}_0^{RL} D_t^{\alpha-1} y'(t)\right)\cdot {}_0^C D_t^{\alpha} y(t)\\
&= {}_0^{RL} D_t^{1-\alpha}\left({}_0^C D_t^{\alpha} y(t)\right)\cdot {}_0^C D_t^{\alpha} y(t)\\
&= {}_0^C D_t^{1-\alpha}\left({}_0^C D_t^{\alpha} y(t)\right)\cdot {}_0^C D_t^{\alpha} y(t)\\
&= \frac{1}{2}{}_0^C D_t^{1-\alpha}\left(\left({}_0^C D_t^{\alpha} y(t)\right)^2\right) + G\left[{}_0^C D_t^{\alpha} y\right](1-\alpha,t)\\
&= \frac{1}{2}{}_0^{RL} D_t^{1-\alpha}\left(\left({}_0^C D_t^{\alpha} y(t)\right)^2\right) + G\left[{}_0^C D_t^{\alpha} y\right](1-\alpha,t)\\
&= \frac{1}{2}\frac{d}{dt}{}_0^{RL} D_t^{-\alpha}\left(\left({}_0^C D_t^{\alpha} y(t)\right)^2\right) + G\left[{}_0^C D_t^{\alpha} y\right](1-\alpha,t).
\end{aligned}
$$

Hence, the conclusion holds. □

Lemma 2 *Let the function $y(t)\in C^1([0,T])$. If $0<\alpha<1$, then it holds that*

$$
\int_0^t {}_0^C D_\tau^{\alpha} y(\tau)d\tau = {}_0^{RL} D_t^{\alpha-1} y(t) - \frac{t^{1-\alpha}}{\Gamma(2-\alpha)} y(0).
$$

Proof According to the property of the semigroup of the RL fractional integral, we obtain

$$
\begin{aligned}
\int_0^t {}_0^C D_s^{\alpha} y(s)ds &= {}_0^{RL} D_t^{-1}\left({}_0^{RL} D_t^{\alpha-1} y'(t)\right) = {}_0^{RL} D_t^{\alpha-1}\left({}_0^{RL} D_t^{-1} y'(t)\right)\\
&= {}_0^{RL} D_t^{\alpha-1} y(t) - {}_0^{RL} D_t^{\alpha-1} y(0)\\
&= {}_0^{RL} D_t^{\alpha-1} y(t) - \frac{t^{1-\alpha}}{\Gamma(2-\alpha)} y(0). \qquad (23)
\end{aligned}
$$

□

For the solution $u(x,t)$ of the normalized fractional DPL equations in a double-layered nanoscale thin film (10)–(16), we have an energy estimation as shown in the following theorem. For simplicity, we first define an energy function

$$
\begin{aligned}
E_1(t) &= \frac{1}{\gamma_1 K_{\mathrm{n},1}}\left(u^2(0,t) + \frac{B_1^{\beta}}{\Gamma(1+\beta)}{}_0^{RL} D_t^{-\beta}\left({}_0^C D_t^{\beta} u(0,t)\right)^2\right)\\
&\quad + \int_0^{l_x}\left(u_x^2(x,t) + \frac{B_1^{\beta}}{\Gamma(1+\beta)}{}_0^{RL} D_t^{-\beta}\left({}_0^C D_t^{\beta} u_x(x,t)\right)^2\right)dx, \quad 0<t\le L_t.\\
E_2(t) &= \frac{1}{\gamma_2 K_{\mathrm{n},2}}\left(u^2(L_x,t) + \frac{B_2^{\beta}}{\Gamma(1+\beta)}{}_0^{RL} D_t^{-\beta}\left({}_0^C D_t^{\beta} u(L_x,t)\right)^2\right)\\
&\quad + \int_{l_x}^{L_x}\left(u_x^2(x,t) + \frac{B_2^{\beta}}{\Gamma(1+\beta)}{}_0^{RL} D_t^{-\beta}\left({}_0^C D_t^{\beta} u_x(x,t)\right)^2\right)dx, \quad 0<t\le L_t\\
E(t) &= \frac{K_{\mathrm{n},1}^2}{6\eta_1}E_1(t) + \frac{K_{\mathrm{n},2}^2}{6\eta_2}E_2(t), \quad 0<t\le L_t.
\end{aligned}
$$

Theorem 1 *Let $u(x,t)$ be the solution of the normalized time fractional DPL model (10)–(16), subject to the homogeneous boundary conditions, i.e., $\phi_1(t)\equiv 0$ and $\phi_2(t)\equiv 0$. Then, it holds that*

$$
E(t) \le E(0) + \frac{t^{1-\alpha}}{2\Gamma(2-\alpha)}\cdot\left(\frac{\eta_1^{\alpha}}{\Gamma(1+\alpha)}\int_0^{l_x}\psi_2^2(x)dx + \frac{\eta_2^{\alpha}}{\Gamma(1+\alpha)}\int_{l_x}^{L_x}\psi_2^2(x)dx\right)
$$

$$+\frac{1}{4}\int_0^t\Big(\int_0^{l_x}F_1^2(x,s)dx+\int_{l_x}^{L_x}F_2^2(x,s)dx\Big)ds,\quad 0<t\le L_t. \tag{24}$$

Proof Multiplying (10) by $u_t(x,t)$ and integrating the result with respect to the variable x from 0 to l_x, we have

$$\begin{aligned}&\int_0^{l_x}u_t^2(x,t)dx+\frac{\eta_1^\alpha}{\Gamma(1+\alpha)}\int_0^{l_x}u_t(x,t)\cdot{}_0^C D_t^{\alpha+1}u(x,t)dx\\&=\frac{K_{\mathrm{n},1}^2}{3\eta_1}\int_0^{l_x}u_t(x,t)\Big(u+\frac{B_1^\beta}{\Gamma(1+\beta)}{}_0^C D_t^\beta u\Big)_{xx}(x,t)dx\\&\quad+\int_0^{l_x}u_t(x,t)\cdot F_1(x,t)dx,\quad 0<t\le L_t.\end{aligned} \tag{25}$$

By virtue of the relation (22), we obtain the inequality

$$\int_0^{l_x}u_t(x,t)\cdot{}_0^C D_t^{\alpha+1}u(x,t)dx\ge\frac{1}{2}{}_0^C D_t^\alpha\Big(\int_0^{l_x}u_t^2(x,t)dx\Big). \tag{26}$$

Applying the integration by parts, then noticing the boundary condition (14) and Lemma 1, it holds that

$$\begin{aligned}&\int_0^{l_x}u_t(x,t)\cdot\Big(u+\frac{B_1^\beta}{\Gamma(1+\beta)}{}_0^C D_t^\beta u\Big)_{xx}(x,t)dx\\&=\Big(u_t\cdot\Big(u+\frac{B_1^\beta}{\Gamma(1+\beta)}{}_0^C D_t^\beta u\Big)_x\Big)(x,t)\Big|_{x=0}^{l_x-0}\\&\quad-\int_0^{l_x}u_{xt}(x,t)\cdot\Big(u+\frac{B_1^\beta}{\Gamma(1+\beta)}{}_0^C D_t^\beta u\Big)_x(x,t)dx\\&\le u_t(l_x-0,t)\cdot\Big(u+\frac{B_1^\beta}{\Gamma(1+\beta)}{}_0^C D_t^\beta u\Big)_x(l_x-0,t)-\frac{1}{2}\frac{d}{dt}E_1(t).\end{aligned} \tag{27}$$

Substituting (26)–(27) into (25) and using the Cauchy–Schwarz inequality with a suitable parameter yield

$$\begin{aligned}&\frac{\eta_1^\alpha}{2\Gamma(1+\alpha)}{}_0^C D_t^\alpha\Big(\int_0^{l_x}u_t^2(x,t)dx\Big)+\frac{K_{\mathrm{n},1}^2}{6\eta_1}\frac{d}{dt}E_1(t)\\&\le\frac{K_{\mathrm{n},1}^2}{3\eta_1}u_t(l_x-0,t)\cdot\Big(u+\frac{B_1^\beta}{\Gamma(1+\beta)}{}_0^C D_t^\beta u\Big)_x(l_x-0,t)\\&\quad+\frac{1}{4}\int_0^{l_x}F_1^2(x,t)dx,\quad 0<t\le L_t.\end{aligned} \tag{28}$$

Similarly, multiplying (11) by $u_t(x,t)$ and integrating the result with respect to the variable x from l_x to L_x, we get

$$\begin{aligned}&\int_{l_x}^{L_x}u_t^2(x,t)dx+\frac{\eta_2^\alpha}{\Gamma(1+\alpha)}\int_{l_x}^{L_x}u_t(x,t)\cdot{}_0^C D_t^{\alpha+1}u(x,t)dx\\&=\frac{K_{\mathrm{n},2}^2}{3\eta_2}\int_{l_x}^{L_x}u_t(x,t)\Big(u+\frac{B_2^\beta}{\Gamma(1+\beta)}{}_0^C D_t^\beta u\Big)_{xx}(x,t)dx\\&\quad+\int_{l_x}^{L_x}u_t(x,t)\cdot F_2(x,t)dx,\quad 0<t\le L_t.\end{aligned} \tag{29}$$

Using the similar argument as (26) and (27) gives

$$\begin{aligned}&\frac{\eta_2^\alpha}{2\Gamma(1+\alpha)}{}_0^C D_t^\alpha\Big(\int_{l_x}^{L_x} u_t^2(x,t)dx\Big)+\frac{K_{\mathrm{n},2}^2}{6\eta_2}\frac{d}{dt}E_2(t)\\&\le-\frac{K_{\mathrm{n},2}^2}{3\eta_2}u_t(l_x+0,t)\cdot\Big(u+\frac{B_2^\beta}{\Gamma(1+\beta)}{}_0^C D_t^\beta u\Big)_x(l_x+0,t)\\&\quad+\frac{1}{4}\int_{l_x}^{L_x}F_2^2(x,t)dx,\quad 0<t\le L_t.\end{aligned}\tag{30}$$

Adding (28) and (30) and using the interfacial conditions (12) and (13) yield

$$\begin{aligned}&{}_0^C D_t^\alpha\Big(\frac{\eta_1^\alpha}{2\Gamma(1+\alpha)}\int_0^{l_x}u_t^2(x,t)dx+\frac{\eta_2^\alpha}{2\Gamma(1+\alpha)}\int_{l_x}^{L_x}u_t^2(x,t)dx\Big)\\&\quad+\frac{dE(t)}{dt}\le\frac{1}{4}\Big[\int_0^{l_x}F_1^2(x,t)dx+\int_{l_x}^{L_x}F_2^2(x,t)dx\Big].\end{aligned}\tag{31}$$

Replacing the variable t with s on both sides of (31), integrating the result with respect to the variable s from 0 to t, and then using Lemma 2, we arrive at

$$\begin{aligned}&{}_0^{RL}D_t^{\alpha-1}\Big(\frac{\eta_1^\alpha}{2\Gamma(1+\alpha)}\int_0^{l_x}u_t^2(x,t)dx+\frac{\eta_2^\alpha}{2\Gamma(1+\alpha)}\int_{l_x}^{L_x}u_t^2(x,t)dx\Big)+E(t)\\&\le\frac{t^{1-\alpha}}{\Gamma(2-\alpha)}\Big(\frac{\eta_1^\alpha}{2\Gamma(1+\alpha)}\int_0^{l_x}\psi_2^2(x)dx+\frac{\eta_2^\alpha}{2\Gamma(1+\alpha)}\int_{l_x}^{L_x}\psi_2^2(x)dx\Big)\\&\quad+E(0)+\frac{1}{4}\int_0^t\Big[\int_0^{l_x}F_1^2(x,s)dx+\int_{l_x}^{L_x}F_2^2(x,s)dx\Big]ds.\end{aligned}\tag{32}$$

Hence, the conclusion holds. □

4 Numerical Method for the Fractional DPL Model

4.1 Discrete Approximations

Divide the interval $[0, L_t]$ into N-subintervals with $\tau=\frac{L_t}{N}$ and $t_k=k\tau$, $0\le k\le N$. Suppose that $u=(u^0,u^1,\cdots,u^N)$ be a grid function defined on $\Omega_\tau\equiv\{t_k\mid 0\le k\le N\}$. For simplicity, we denote a difference quotient operator and an average operator in time,

$$\delta_t u^{k-\frac{1}{2}}=\frac{1}{\tau}(u^k-u^{k-1}),\quad u^{k-\frac{1}{2}}=\frac{1}{2}(u^k+u^{k-1}),$$

and some fractional numerical differentiation operators (called $L1$ formula [30]) for the Caputo fractional derivatives as follows,

$$\delta_\tau^\beta u^k=\frac{\tau^{-\beta}}{\Gamma(2-\beta)}\Big[a_0^{(\beta)}u^k-\sum_{\ell=1}^{k-1}(a_{k-\ell-1}^{(\beta)}-a_{k-\ell}^{(\beta)})u^\ell-a_{k-1}^{(\beta)}u^0\Big],\tag{33}$$

$$\delta_\tau^\beta u^{k-\frac{1}{2}}=\frac{\tau^{-\beta}}{\Gamma(2-\beta)}\Big[a_0^{(\beta)}u^{k-\frac{1}{2}}-\sum_{\ell=1}^{k-1}(a_{k-\ell-1}^{(\beta)}-a_{k-\ell}^{(\beta)})u^{\ell-\frac{1}{2}}-a_{k-1}^{(\beta)}u^0\Big],\tag{34}$$

$$\Delta_\tau^\alpha(\delta_t u^{k-\frac{1}{2}}, q) = \frac{\tau^{-\alpha}}{\Gamma(2-\alpha)}\Big[a_0^{(\alpha)}\delta_t u^{k-\frac{1}{2}} - \sum_{\ell=1}^{k-1}(a_{k-\ell-1}^{(\alpha)} - a_{k-\ell}^{(\alpha)})\delta_t u^{\ell-\frac{1}{2}} - a_{k-1}^{(\alpha)} q\Big], \quad (35)$$

where q is a given value, and the coefficients

$$a_\ell^{(\zeta)} = (\ell+1)^{1-\zeta} - \ell^{1-\zeta}, \quad \ell \geq 0, \quad 0 < \zeta = \alpha, \beta < 1. \quad (36)$$

From the above definition, it is obvious that $\{a_\ell^{(\zeta)}\}_{\ell=0}^{\infty}$ is a nonnegative and descending series, i.e.,

$$a_\ell^{(\zeta)} \geq 0 \quad (\ell \geq 0); \quad a_\ell^{(\zeta)} - a_{\ell-1}^{(\zeta)} \leq 0 \quad (\ell \geq 1).$$

We then list the truncation errors of the $L1$ formulas in the following lemma.

Lemma 3 [30] *Suppose $f(t) \in C^2[0, t_n]$ and $0 < \alpha, \beta < 1$. We have*

$$\frac{1}{2}\Big[{}_0^C D_t^\beta f(t_k) + {}_0^C D_t^\beta f(t_{k-1})\Big] = \delta_\tau^\beta f^{k-\frac{1}{2}} + O(\tau^{2-\beta}),$$

and

$$\frac{1}{2}\Big[{}_0^C D_t^{\alpha+1} f(t_k) + {}_0^C D_t^{\alpha+1} f(t_{k-1})\Big] = \Delta_\tau^\alpha(\delta_t f^{k-\frac{1}{2}}, f'(0)) + O(\tau^{2-\alpha}),$$

where $f = (f^0, f^1, f^2, \cdots, f^N)$ and each component $f^k \equiv f(t_k)$, $0 \leq k \leq N$.

For the numerical approximation of the first order temporal derivative, a lemma is prepared below.

Lemma 4 [31] *Suppose $f(t) \in C^3[t_{k-1}, t_k]$ and denote $t_{k-\frac{1}{2}} = \frac{1}{2}(t_{k-1} + t_k)$, then it holds*

$$\frac{1}{2}\big[f'(t_k) + f'(t_{k-1})\big] = \frac{f(t_k) - f(t_{k-1})}{\tau} + \frac{\tau^2}{16}\int_0^1 \Big[f'''\big(t_{k-\frac{1}{2}} + \frac{\tau}{2}\theta\big) + f'''\big(t_{k-\frac{1}{2}} - \frac{\tau}{2}\theta\big)\Big](1-\theta^2)ds.$$

Next, we introduce some discrete notations in space. Take two positive integers m and M $(m < M)$. Let $h_1 = \frac{l_x}{m}$, $\omega_l = \{i \mid 0 \leq i \leq m\}$, $\Omega_{h,l} = \{x_i \mid x_i = ih_1,\ i \in \omega_l\}$ and $h_2 = \frac{L_x - l_x}{M-m}$, $\omega_r = \{i \mid m \leq i \leq M\}$, $\Omega_{h,r} = \{x_i \mid x_i = x_m + (i-m)h_2,\ i \in \omega_r\}$, as shown in Fig. 1. Let $\mathscr{U}_h = \{u \mid u = (u_0, u_1, \cdots, u_M)\}$ be the grid function space defined on $\Omega_h = \Omega_{h,l} \cup \Omega_{h,r}$. For any $u, v \in \mathscr{U}_h$, we have

$$\delta_x u_{i-\frac{1}{2}} = \frac{1}{h_1}(u_i - u_{i-1}), \quad i \in \omega_l \backslash \{0\}; \quad \delta_x u_{i-\frac{1}{2}} = \frac{1}{h_2}(u_i - u_{i-1}), \quad i \in \omega_r \backslash \{m\};$$

$$(u, v)_l = h_1\Big(\frac{1}{2}u_0 v_0 + \sum_{i=1}^{m-1} u_i v_i + \frac{1}{2}u_m v_m\Big), \quad \|u\|_l = \sqrt{(u, u)_l};$$

$$(u, v)_r = h_2\Big(\frac{1}{2}u_m v_m + \sum_{i=m+1}^{M-1} u_i v_i + \frac{1}{2}u_M v_M\Big), \quad \|u\|_r = \sqrt{(u, u)_r};$$

$$(\delta_x u, \delta_x v)_l = h_1 \sum_{i=1}^{m} \big(\delta_x u_{i-\frac{1}{2}}\big)\delta_x v_{i-\frac{1}{2}}, \quad \|\delta_x u\|_l = \sqrt{(\delta_x u, \delta_x u)_l};$$

$$(\delta_x u, \delta_x v)_r = h_2 \sum_{i=m+1}^{M} \big(\delta_x u_{i-\frac{1}{2}}\big)\delta_x v_{i-\frac{1}{2}}, \quad \|\delta_x u\|_r = \sqrt{(\delta_x u, \delta_x u)_r};$$
$$\|u\|_{l,\infty} = \max_{0\le i\le m} |u_i|, \quad \|u\|_{r,\infty} = \max_{m\le i\le M} |u_i|.$$

For any $u \in \mathscr{U}_h$, we denote

$$\delta_x^2 u_i = \begin{cases} \frac{2}{h_1}(\delta_x u_{\frac{1}{2}} - \frac{1}{\gamma_1 K_{\mathrm{n},1}} u_0), & i = 0, \\ \frac{1}{h_1}(\delta_x u_{i+\frac{1}{2}} - \delta_x u_{i-\frac{1}{2}}), & 1 \le i \le m-1, \end{cases} \tag{37}$$

and

$$\delta_x^2 u_i = \begin{cases} \frac{1}{h_2}(\delta_x u_{i+\frac{1}{2}} - \delta_x u_{i-\frac{1}{2}}), & m+1 \le i \le M-1, \\ \frac{2}{h_2}(-\frac{1}{\gamma_2 K_{\mathrm{n},2}} u_M - \delta_x u_{M-\frac{1}{2}}), & i = M. \end{cases} \tag{38}$$

Lemma 5 *Let c and h be two given constants and $h > 0$.*

(I) *Suppose $g(x) \in C^3[c, c+h]$, then it holds that*

$$g''(c) = \frac{2}{h}\left[\frac{g(c+h) - g(c)}{h} - g'(c)\right] - h\int_0^1 g'''(c+\theta h)(1-\theta)^2 d\theta;$$

(II) *Suppose $g(x) \in C^3[c-h, c]$, then it holds that*

$$g''(c) = \frac{2}{h}\left[g'(c) - \frac{g(c) - g(c-h)}{h}\right] + h\int_0^1 g'''(c-\theta h)(1-\theta)^2 d\theta;$$

(III) *Suppose $g(x) \in C^4[c-h, c+h]$, then it holds that*

$$g''(c) = \frac{1}{h^2}[g(c+h) - 2g(c) + g(c-h)] - \frac{h^2}{6}\int_0^1 [g^{(4)}(c-\theta h) + g^{(4)}(c+\theta h)](1-\theta)^3 d\theta.$$

Proof The conclusions (I)–(III) are easy to achieve by applying the Taylor expansion with the integral remainder term for the smooth function $g(x)$. □

4.2 Finite Difference Scheme

From now on, we will construct a discretization scheme for the problem (10)–(16). The derivation of the scheme adopts the tactic that the semi-discretization of the spatial derivative is prior to the approximation of the temporal derivative. Let $u(x,t)$ be the solution of (10)–(16). Denote the discrete functions by

$$\begin{aligned} U_i(t) &= u(x_i, t),\ i \in \omega_l \cup \omega_r;\ (F_1)_i(t) = F_1(x_i, t),\ i \in \omega_l;\ (F_2)_i(t) \\ &= F_2(x_i, t),\ i \in \omega_r;\ 0 \le t \le L_t; \\ U_i^k &= u(x_i, t_k),\ i \in \omega_l \cup \omega_r;\ (F_1)_i^k = F_1(x_i, t_k),\ i \in \omega_l;\ (F_2)_i^k \\ &= F_2(x_i, t_k),\ i \in \omega_r;\ 0 \le k \le N; \end{aligned}$$

and $\varphi_i = \varphi(x_i)$, $\psi_i = \psi(x_i)$, $i \in \omega_l \cup \omega_r$.

For the sake of brevity in writing the scheme, we firstly introduce several functions with respect to the variable t, i.e.,

$$(G_1)_i(t) = \begin{cases} \frac{2K_{\mathrm{n},1}}{3\gamma_1\eta_1 h_1}\Big(\phi_1(t) + \frac{B_1^\beta}{\Gamma(1+\beta)}{}_0^C D_t^\beta \phi_1(t)\Big) + (F_1)_0(t), & i = 0, \\ (F_1)_i(t), & 1 \le i \le m-1, \\ \frac{h_1}{h_1+h_2}(F_1)_m(t), & i = m; \end{cases} \tag{39}$$

$$(G_2)_i(t) = \begin{cases} \frac{h_2}{h_1+h_2}(F_2)_m(t), & i = m, \\ (F_2)(t), & m+1 \le i \le M-1, \\ \frac{2K_{\mathrm{n},2}}{3\gamma_2\eta_2 h_2}\Big(\phi_2(t) + \frac{B_2^\beta}{\Gamma(1+\beta)}{}_0^C D_t^\beta \phi_2(t)\Big) + (F_2)_M(t), & i = M; \end{cases} \tag{40}$$

$$r_i(t) = \begin{cases} -\frac{K_{\mathrm{n},1}^2}{3\eta_1}\int_0^1 \Big(u + \frac{B_1^\beta}{\Gamma(1+\beta)}{}_0^C D_t^\beta u\Big)_{xxx}(x_0+\theta h_1, t)(1-\theta)^2 d\theta, & i = 0, \\ -\frac{1}{6}\frac{K_{\mathrm{n},1}^2}{3\eta_1}\int_0^1 \Big[\Big(u + \frac{B_1^\beta}{\Gamma(1+\beta)}{}_0^C D_t^\beta u\Big)_{xxxx}(x_i - \theta h_1, t) \\ \quad + \Big(u + \frac{B_1^\beta}{\Gamma(1+\beta)}{}_0^C D_t^\beta u\Big)_{xxxx}(x_i + \theta h_1, t)\Big](1-\theta)^3 d\theta, & 1 \le i \le m-1, \\ \frac{K_{\mathrm{n},1}^2}{3\eta_1}\int_0^1 \Big(u + \frac{B_1^\beta}{\Gamma(1+\beta)}{}_0^C D_t^\beta u\Big)_{xxx}(x_m - \theta h_1, t)(1-\theta)^2 d\theta, & i = m; \end{cases} \tag{41}$$

and

$$s_i(t) = \begin{cases} -\frac{K_{\mathrm{n},2}^2}{3\eta_2}\int_0^1 \Big(u + \frac{B_2^\beta}{\Gamma(1+\beta)}{}_0^C D_t^\beta u\Big)_{xxx}(x_m + \theta h_2, t)(1-\theta)^2 d\theta, & i = m, \\ -\frac{1}{6}\frac{K_{\mathrm{n},2}^2}{3\eta_2}\int_0^1 \Big[\Big(u + \frac{B_2^\beta}{\Gamma(1+\beta)}{}_0^C D_t^\beta u\Big)_{xxxx}(x_i - \theta h_2, t) \\ \quad + \Big(u + \frac{B_2^\beta}{\Gamma(1+\beta)}{}_0^C D_t^\beta u\Big)_{xxxx}(x_i + \theta h_2, t)\Big](1-\theta)^3 d\theta, & m+1 \le i \le M-1, \\ \frac{K_{\mathrm{n},2}^2}{3\eta_2}\int_0^1 \Big(u + \frac{B_2^\beta}{\Gamma(1+\beta)}{}_0^C D_t^\beta u\Big)_{xxx}(x_M - \theta h_2, t)(1-\theta)^2 d\theta, & i = M. \end{cases} \tag{42}$$

Let us begin by considering (10) at $(x_i, t) \in \{\Omega_{h,l}\backslash x_m\} \times (0, L_t]$. According to Lemma 5 and the left boundary condition (14), a semi-discretization scheme reads

$$\frac{d}{dt}U_0(t) + \frac{\eta_1^\alpha}{\Gamma(1+\alpha)}{}_0^C D_t^{\alpha+1} U_0(t) = \frac{K_{\mathrm{n},1}^2}{3\eta_1}\delta_x^2\Big(U_0(t) + \frac{B_1^\beta}{\Gamma(1+\beta)} \cdot {}_0^C D_t^\beta U_0(t)\Big) + (G_1)_0(t) + h_1 \cdot r_0(t), \quad i = 0, \tag{43}$$

$$\frac{d}{dt}U_i(t) + \frac{\eta_1^\alpha}{\Gamma(1+\alpha)}{}_0^C D_t^{\alpha+1} U_i(t) = \frac{K_{\mathrm{n},1}^2}{3\eta_1}\delta_x^2\Big(U_i(t) + \frac{B_1^\beta}{\Gamma(1+\beta)} \cdot {}_0^C D_t^\beta U_i(t)\Big) + (G_1)_i(t) + h_1^2 \cdot r_i(t), \quad 1 \le i \le m-1. \tag{44}$$

We then move on to consider (11) at $(x_i, t) \in \{\Omega_{h,r}\backslash x_m\} \times (0, L_t]$. A similar technique with (43) and (44) yields the following semi-discretization scheme:

$$\frac{d}{dt}U_i(t) + \frac{\eta_2^\alpha}{\Gamma(1+\alpha)}{}_0^C D_t^{\alpha+1} U_i(t) = \frac{K_{\mathrm{n},2}^2}{3\eta_2}\delta_x^2\Big(U_i(t) + \frac{B_2^\beta}{\Gamma(1+\beta)} \cdot {}_0^C D_t^\beta U_i(t)\Big) + (G_2)_i(t) + h_2^2 \cdot s_i(t), \quad m+1 \le i \le M-1, \tag{45}$$

$$\frac{d}{dt}U_M(t)+\frac{\eta_2^\alpha}{\Gamma(1+\alpha)}{}_0^C D_t^{\alpha+1}U_M(t)$$
$$=\frac{K_{\mathrm{n},2}^2}{3\eta_2}\delta_x^2\Big(U_M(t)+\frac{B_2^\beta}{\Gamma(1+\beta)}\cdot{}_0^C D_t^\beta U_M(t)\Big)+(G_2)_M(t)+h_2\cdot s_M(t),\quad i=M. \tag{46}$$

Next, a semi-discretization scheme on the interface is considered. Using Lemma 5 for (10) at (x_m-0,t) and for (11) at (x_m+0,t), respectively, and noticing the interfacial condition (12), we can obtain

$$\frac{d}{dt}U_m(t)+\frac{\eta_1^\alpha}{\Gamma(1+\alpha)}{}_0^C D_t^{\alpha+1}U_m(t)=\frac{K_{\mathrm{n},1}^2}{3\eta_1}\frac{2}{h_1}\Big[\Big(u+\frac{B_1^\beta}{\Gamma(1+\beta)}{}_0^C D_t^\beta u\Big)_x(x_m-0,t)$$
$$-\delta_x\Big(U_{m-\frac12}(t)+\frac{B_1^\beta}{\Gamma(1+\beta)}{}_0^C D_t^\beta U_{m-\frac12}(t)\Big)\Big]+(F_1)_m(t)+h_1\cdot r_m(t), \tag{47}$$
$$\frac{d}{dt}U_m(t)+\frac{\eta_2^\alpha}{\Gamma(1+\alpha)}{}_0^C D_t^{\alpha+1}U_m(t)=\frac{K_{\mathrm{n},2}^2}{3\eta_2}\frac{2}{h_2}\Big[-\Big(u+\frac{B_2^\beta}{\Gamma(1+\beta)}{}_0^C D_t^\beta u\Big)_x(x_m+0,t)$$
$$+\delta_x\Big(U_{m+\frac12}(t)+\frac{B_2^\beta}{\Gamma(1+\beta)}{}_0^C D_t^\beta U_{m+\frac12}(t)\Big)\Big]+(F_2)_m(t)+h_2\cdot s_m(t). \tag{48}$$

Multiplying (47) by $\frac{h_1}{h_1+h_2}$ and (48) by $\frac{h_2}{h_1+h_2}$, respectively, and then adding the results and noticing the interfacial condition (13), we deduce

$$\frac{h_1}{h_1+h_2}\Big[\frac{d}{dt}U_m(t)+\frac{\eta_1^\alpha}{\Gamma(1+\alpha)}{}_0^C D_t^{\alpha+1}U_m(t)\Big]$$
$$+\frac{h_2}{h_1+h_2}\Big[\frac{d}{dt}U_m(t)+\frac{\eta_2^\alpha}{\Gamma(1+\alpha)}{}_0^C D_t^{\alpha+1}U_m(t)\Big]$$
$$=\frac{2}{3(h_1+h_2)}\Big[\frac{K_{\mathrm{n},2}^2}{\eta_2}\delta_x\Big(U_{m+\frac12}(t)+\frac{B_2^\beta}{\Gamma(1+\beta)}{}_0^C D_t^\beta U_{m+\frac12}(t)\Big)$$
$$-\frac{K_{\mathrm{n},1}^2}{\eta_1}\delta_x\Big(U_{m-\frac12}(t)+\frac{B_1^\beta}{\Gamma(1+\beta)}\cdot{}_0^C D_t^\beta U_{m-\frac12}(t)\Big)\Big]$$
$$+(G_1)_m(t)+(G_2)_m(t)+\frac{h_1}{h_1+h_2}h_1\cdot r_m(t)+\frac{h_2}{h_1+h_2}h_2\cdot s_m(t). \tag{49}$$

Further, considering (43)–(46) and (49) at $t=t_{k-1}$ and $t=t_k$, respectively, averaging the results and then using Lemmas 3 and 4, we have

$$\delta_t U_i^{k-\frac12}+\frac{\eta_1^\alpha}{\Gamma(1+\alpha)}\Delta_\tau^\alpha\big(\delta_t U_i^{k-\frac12},\psi_i\big)=\frac{K_{\mathrm{n},1}^2}{3\eta_1}\delta_x^2\Big(U_i^{k-\frac12}+\frac{B_1^\beta}{\Gamma(1+\beta)}\delta_\tau^\beta U_i^{k-\frac12}\Big)+(G_1)_i^{k-\frac12}$$
$$+(R^t)_i^{k-\frac12}+(R^x)_i^{k-\frac12},\quad i\in\omega_l\backslash\{m\},\quad 1\le k\le N, \tag{50}$$
$$\frac{h_1}{h_1+h_2}\Big(\delta_t U_m^{k-\frac12}+\frac{\eta_1^\alpha}{\Gamma(1+\alpha)}\Delta_\tau^\alpha\big(\delta_t U_m^{k-\frac12},\psi_m\big)\Big)$$
$$+\frac{h_2}{h_1+h_2}\Big(\delta_t U_m^{k-\frac12}+\frac{\eta_2^\alpha}{\Gamma(1+\alpha)}\Delta_\tau^\alpha\big(\delta_t U_m^{k-\frac12},\psi_m\big)\Big)$$
$$=\frac{2}{3(h_1+h_2)}\Big[\frac{K_{\mathrm{n},2}^2}{\eta_2}\delta_x\Big(U_{m+\frac12}^{k-\frac12}+\frac{B_2^\beta}{\Gamma(1+\beta)}\delta_\tau^\beta U_{m+\frac12}^{k-\frac12}\Big)$$

$$
\begin{aligned}
&- \frac{K_{\mathrm{n},1}^2}{\eta_1}\delta_x\Big(U_{m-\frac{1}{2}}^{k-\frac{1}{2}} + \frac{B_1^\beta}{\Gamma(1+\beta)}\delta_\tau^\beta U_{m-\frac{1}{2}}^{k-\frac{1}{2}}\Big)\Big] \\
&+ (G_1)_m^{k-\frac{1}{2}} + (G_2)_m^{k-\frac{1}{2}} + \frac{h_1}{h_1+h_2}[(R^t)_m^{k-\frac{1}{2}} + (R^x)_m^{k-\frac{1}{2}}] \\
&+ \frac{h_2}{h_1+h_2}[(S^t)_m^{k-\frac{1}{2}} + (S^x)_m^{k-\frac{1}{2}}], \quad 1 \le k \le N, \qquad (51)\\
&\delta_t U_i^{k-\frac{1}{2}} + \frac{\eta_2^\alpha}{\Gamma(1+\alpha)}\Delta_\tau^\alpha\big(\delta_t U_i^{k-\frac{1}{2}}, \psi_i\big) \\
&= \frac{K_{\mathrm{n},2}^2}{3\eta_2}\delta_x^2\Big(U_i^{k-\frac{1}{2}} + \frac{B_2^\beta}{\Gamma(1+\beta)}\delta_\tau^\beta U_i^{k-\frac{1}{2}}\Big) + (G_2)_i^{k-\frac{1}{2}} \\
&+ (S^t)_i^{k-\frac{1}{2}} + (S^x)_i^{k-\frac{1}{2}}, \quad i \in \omega_r\backslash\{m\}, \quad 1 \le k \le N. \qquad (52)
\end{aligned}
$$

Here the truncation errors satisfy, for $1 \le k \le N$,

$$
\begin{aligned}
&\big|(R^t)_i^{k-\frac{1}{2}}\big| \le c_0\tau^{\min\{2-\alpha,2-\beta\}}, \quad i \in \omega_l; \quad \big|(S^t)_i^{k-\frac{1}{2}}\big| \le c_0\tau^{\min\{2-\alpha,2-\beta\}}, \quad i \in \omega_r; \qquad (53)\\
&\big|(R^x)_i^{k-\frac{1}{2}}\big| = h_1^2\Big|\frac{r_i(t_k)+r_i(t_{k-1})}{2}\Big| \le c_0h_1^2, \quad i \in \omega_l\backslash\{0,m\}; \qquad (54)\\
&\big|(R^x)_i^{k-\frac{1}{2}}\big| = h_1\Big|\frac{r_i(t_k)+r_i(t_{k-1})}{2}\Big| \le c_0h_1, \quad i \in \{0,m\}; \qquad (55)\\
&\big|(S^x)_i^{k-\frac{1}{2}}\big| = h_2^2\Big|\frac{s_i(t_k)+s_i(t_{k-1})}{2}\Big| \le c_0h_2^2, \quad i \in \omega_r\backslash\{m,M\}; \qquad (56)\\
&\big|(S^x)_i^{k-\frac{1}{2}}\big| = h_2\Big|\frac{s_i(t_k)+s_i(t_{k-1})}{2}\Big| \le c_0h_2, \quad i \in \{m,M\}; \qquad (57)
\end{aligned}
$$

and, for $1 \le k \le N-1$,

$$
\begin{aligned}
&\Big|\frac{(R^x)_i^{k+\frac{1}{2}} - (R^x)_i^{k-\frac{1}{2}}}{\tau}\Big| \\
&= \frac{h_1}{2}\Big|\frac{r_i(t_{k+1})-r_i(t_k)}{\tau} + \frac{r_i(t_k)-r_i(t_{k-1})}{\tau}\Big| \le c_0h_1, \quad i \in \{0,m\}; \qquad (58)\\
&\Big|\frac{(S^x)_i^{k+\frac{1}{2}} - (S^x)_i^{k-\frac{1}{2}}}{\tau}\Big| \\
&= \frac{h_2}{2}\Big|\frac{s_i(t_{k+1})-s_i(t_k)}{\tau} + \frac{s_i(t_k)-s_i(t_{k-1})}{\tau}\Big| \le c_0h_2, \quad i \in \{m,M\}, \qquad (59)
\end{aligned}
$$

where c_0 is a positive constant number independent of τ, h_1 and h_2.

Noticing the initial condition,

$$
U_i^0 = \varphi(x_i), \quad i \in \omega_l \cup \omega_r, \qquad (60)
$$

and dropping small terms in (50)–(52), respectively, we obtain a finite difference scheme for the problem (10)–(16) as follows

$$
\begin{aligned}
&\delta_t u_i^{k-\frac{1}{2}} + \frac{\eta_1^\alpha}{\Gamma(1+\alpha)}\Delta_\tau^\alpha\big(\delta_t u_i^{k-\frac{1}{2}}, \psi_i\big) = \frac{K_{\mathrm{n},1}^2}{3\eta_1}\delta_x^2\Big(u_i^{k-\frac{1}{2}} + \frac{B_1^\beta}{\Gamma(1+\beta)}\delta_\tau^\beta u_i^{k-\frac{1}{2}}\Big) + (G_1)_i^{k-\frac{1}{2}}, \\
&\quad i \in \omega_l\backslash\{m\}, \quad 1 \le k \le N, \qquad (61)\\
&\frac{h_1}{h_1+h_2}\Big(\delta_t u_m^{k-\frac{1}{2}} + \frac{\eta_1^\alpha}{\Gamma(1+\alpha)}\Delta_\tau^\alpha\big(\delta_t u_m^{k-\frac{1}{2}}, \psi_m\big)\Big)
\end{aligned}
$$

$$
\begin{aligned}
&+\frac{h_2}{h_1+h_2}\Big(\delta_t u_m^{k-\frac{1}{2}}+\frac{\eta_2^\alpha}{\Gamma(1+\alpha)}\Delta_\tau^\alpha\big(\delta_t u_m^{k-\frac{1}{2}},\psi_m\big)\Big)\\
&=\frac{2}{3(h_1+h_2)}\Bigg[\frac{K_{\mathrm{n},2}^2}{\eta_2}\delta_x\Big(u_{m+\frac{1}{2}}^{k-\frac{1}{2}}+\frac{B_2^\beta}{\Gamma(1+\beta)}\delta_\tau^\beta u_{m+\frac{1}{2}}^{k-\frac{1}{2}}\Big)\\
&\quad-\frac{K_{\mathrm{n},1}^2}{\eta_1}\delta_x\Big(u_{m-\frac{1}{2}}^{k-\frac{1}{2}}+\frac{B_1^\beta}{\Gamma(1+\beta)}\delta_\tau^\beta u_{m-\frac{1}{2}}^{k-\frac{1}{2}}\Big)\Bigg]\\
&\quad+(G_1)_m^{k-\frac{1}{2}}+(G_2)_m^{k-\frac{1}{2}},\quad 1\le k\le N,
\end{aligned}
\tag{62}
$$

$$
\delta_t u_i^{k-\frac{1}{2}}+\frac{\eta_2^\alpha}{\Gamma(1+\alpha)}\Delta_\tau^\alpha\big(\delta_t u_i^{k-\frac{1}{2}},\psi_i\big)=\frac{K_{\mathrm{n},2}^2}{3\eta_2}\delta_x^2\Big(u_i^{k-\frac{1}{2}}+\frac{B_2^\beta}{\Gamma(1+\beta)}\delta_\tau^\beta u_i^{k-\frac{1}{2}}\Big)+(G_2)_i^{k-\frac{1}{2}},
$$

$$
i\in\omega_r\backslash\{m\},\quad 1\le k\le N,
\tag{63}
$$

$$
u_i^0=\varphi_i,\quad i\in\omega_l\cup\omega_r.
\tag{64}
$$

Let $u^n=(u_0^n,u_1^n,\cdots,u_m^n,\cdots,u_{M-1}^n,u_M^n)^T$, $v^n=(v_0^n,v_1^n,\cdots,v_m^n,\cdots,v_{M-1}^n,v_M^n)^T$, $n=0,1,\cdots,N$. The scheme (61)–(64) can be written in the following matrix form:

$$
\begin{cases}
Av^n=\sum_{j=1}^{n-1}A_{n-j+1}v^j+Bu^{n-1}+b^n,\\
u^n=u^{n-1}+\tau v^n,
\end{cases}
\qquad n=1,2,\cdots,N.
\tag{65}
$$

The coefficient matrix A is strictly diagonally dominant. Hence, the presented scheme (61)–(64) has a unique solution and can be easily solved using the Thomas algorithm.

5 Stability and Convergence of the Scheme

In this section, we will analyze the stability and convergence of the presented scheme (61)–(64) for the normalized time fractional DPL equations in a double-layered nanoscale thin film (10)–(16). Prior to this, some useful lemmas will be listed in preparation for the theoretical analysis.

Lemma 6 *Let $\Delta_\tau^\alpha(\delta_t y^{k-\frac{1}{2}},q)$ be defined in (35). Then we have*

$$
\begin{aligned}
&\big(\Delta_\tau^\alpha(\delta_t y^{k-\frac{1}{2}},q)\big)\cdot\delta_t y^{k-\frac{1}{2}}\\
&\ge\frac{1}{\tau}\Bigg[\frac{\tau^{1-\alpha}}{2\Gamma(2-\alpha)}\sum_{\ell=1}^{k}a_{k-\ell}^{(\alpha)}(\delta_t y^{\ell-\frac{1}{2}})^2-\frac{\tau^{1-\alpha}}{2\Gamma(2-\alpha)}\sum_{\ell=1}^{k-1}a_{k-1-\ell}^{(\alpha)}(\delta_t y^{\ell-\frac{1}{2}})^2\Bigg]\\
&\quad+\Big(\frac{1}{2}-\epsilon\Big)\frac{\tau^{-\alpha}}{\Gamma(2-\alpha)}a_{k-1}^{(\alpha)}(\delta_t y^{k-\frac{1}{2}})^2-\frac{1}{4\epsilon}\frac{\tau^{-\alpha}}{\Gamma(2-\alpha)}a_{k-1}^{(\alpha)}q^2,
\end{aligned}
$$

where $0<\epsilon\le\frac{1}{2}$.

Proof An immediate application of the Cauchy–Schwarz inequality for the fractional numerical differentiation operator $\Delta_\tau^\alpha(\delta_t y^{k-\frac{1}{2}},q)$ leads to the following estimate

$$
\begin{aligned}
&\big(\Delta_\tau^\alpha(\delta_t y^{k-\frac{1}{2}},q)\big)\cdot\delta_t y^{k-\frac{1}{2}}\\
&=\frac{\tau^{-\alpha}}{\Gamma(2-\alpha)}\Big[a_0^{(\alpha)}\delta_t y^{k-\frac{1}{2}}-\sum_{\ell=1}^{k-1}\big(a_{k-\ell-1}^{(\alpha)}-a_{k-\ell}^{(\alpha)}\big)\delta_t y^{\ell-\frac{1}{2}}-a_{k-1}^{(\alpha)}q\Big]\cdot\delta_t y^{k-\frac{1}{2}}\\
&\geq\frac{\tau^{-\alpha}}{\Gamma(2-\alpha)}\Big[a_0^{(\alpha)}(\delta_t y^{k-\frac{1}{2}})^2-\sum_{\ell=1}^{k-1}(a_{k-\ell-1}^{(\alpha)}-a_{k-\ell}^{(\alpha)})\frac{(\delta_t y^{k-\frac{1}{2}})^2+(\delta_t y^{\ell-\frac{1}{2}})^2}{2}\\
&\quad-a_{k-1}^{(\alpha)}\Big(\epsilon(\delta_t y^{k-\frac{1}{2}})^2+\frac{1}{4\epsilon}q^2\Big)\Big]\\
&=\frac{1}{\tau}\Big[\frac{\tau^{1-\alpha}}{2\Gamma(2-\alpha)}\sum_{\ell=1}^{k}a_{k-\ell}^{(\alpha)}(\delta_t y^{\ell-\frac{1}{2}})^2-\frac{\tau^{1-\alpha}}{2\Gamma(2-\alpha)}\sum_{\ell=1}^{k-1}a_{k-1-\ell}^{(\alpha)}(\delta_t y^{\ell-\frac{1}{2}})^2\Big]\\
&\quad+\Big(\frac{1}{2}-\epsilon\Big)\frac{\tau^{-\alpha}}{\Gamma(2-\alpha)}a_{k-1}^{(\alpha)}(\delta_t y^{k-\frac{1}{2}})^2-\frac{1}{4\epsilon}\frac{\tau^{-\alpha}}{\Gamma(2-\alpha)}a_{k-1}^{(\alpha)}q^2,
\end{aligned}
$$

where ϵ is a positive constant and $\epsilon\leq\frac{1}{2}$. Hence, the conclusion holds. □

Lemma 7 *Let $\delta_\tau^\beta y^{k-\frac{1}{2}}$ be defined in (34). Then we have*

$$\sum_{k=1}^{N}(\delta_\tau^\beta y^{k-\frac{1}{2}})\cdot\delta_t y^{k-\frac{1}{2}}\geq 0.$$

Proof According to the definition of the fractional numerical differentiation operator $\delta_\tau^\beta y^{k-\frac{1}{2}}$, we point out [19]

$$
\begin{aligned}
\delta_\tau^\beta y^{k-\frac{1}{2}}&=\frac{\delta_\tau^\beta y^k+\delta_\tau^\beta y^{k-1}}{2}=\frac{1}{2}\Big[\frac{\tau^{1-\beta}}{\Gamma(2-\beta)}\sum_{\ell=1}^{k}a_{k-\ell}^{(\beta)}\delta_t y^{\ell-\frac{1}{2}}\\
&\quad+\frac{\tau^{1-\beta}}{\Gamma(2-\beta)}\sum_{\ell=1}^{k-1}a_{k-1-\ell}^{(\beta)}\delta_t y^{\ell-\frac{1}{2}}\Big].
\end{aligned}
$$

Then, from [32], it holds that

$$
\begin{aligned}
\sum_{k=1}^{N}(\delta_\tau^\beta y^{k-\frac{1}{2}})\cdot\delta_t y^{k-\frac{1}{2}}&=\frac{1}{2}\frac{\tau^{1-\beta}}{\Gamma(2-\beta)}\Big[\sum_{k=1}^{N}\sum_{\ell=1}^{k}a_{k-\ell}^{(\beta)}\delta_t y^{\ell-\frac{1}{2}}\cdot\delta_t y^{k-\frac{1}{2}}\\
&\quad+\sum_{k=1}^{N}\sum_{\ell=1}^{k-1}a_{k-1-\ell}^{(\beta)}\delta_t y^{\ell-\frac{1}{2}}\cdot\delta_t y^{k-\frac{1}{2}}\Big]\geq 0.
\end{aligned}
$$

Hence, the conclusion holds. □

Lemma 8 *Suppose that $u\in\mathcal{U}_h$, then for any $\epsilon>0$, it holds that*

$$
\begin{aligned}
\|u\|_{l,\infty}^2&\leq(1+\epsilon)u_0^2+\Big(1+\frac{1}{\epsilon}\Big)l_x\|\delta_x u\|_l^2,\\
\|u\|_{r,\infty}^2&\leq(1+\epsilon)u_M^2+\Big(1+\frac{1}{\epsilon}\Big)(L_x-l_x)\|\delta_x u\|_r^2,
\end{aligned}
$$

where ϵ is an any positive constant.

Proof Notice

$$u_i = u_0 + \sum_{j=1}^{i}(u_j - u_{j-1}) = u_0 + h_1 \sum_{j=1}^{i} \delta_x u_{j-\frac{1}{2}}, \quad 0 \le i \le m, \tag{66}$$

$$u_i = u_M - \sum_{j=i+1}^{M}(u_j - u_{j-1}) = u_M - h_2 \sum_{j=i+1}^{M} \delta_x u_{j-\frac{1}{2}}, \quad m \le i \le M. \tag{67}$$

Squaring both sides of (66) and using the Cauchy–Schwarz inequality, we have

$$\begin{aligned} u_i^2 &= \Big(u_0 + h_1 \sum_{j=1}^{i} \delta_x u_{j-\frac{1}{2}}\Big)^2 \\ &\le (1+\epsilon)u_0^2 + \Big(1+\frac{1}{\epsilon}\Big)\Big(h_1 \sum_{j=1}^{i} \delta_x u_{j-\frac{1}{2}}\Big)^2 \\ &\le (1+\epsilon)u_0^2 + \Big(1+\frac{1}{\epsilon}\Big) l_x \|\delta_x u\|_l^2, \quad 0 \le i \le m. \end{aligned} \tag{68}$$

Similarly, it follows from (67) that

$$u_i^2 \le (1+\epsilon)u_M^2 + \Big(1+\frac{1}{\epsilon}\Big)(L_x - l_x)\|\delta_x u\|_r^2, \quad m \le i \le M. \tag{69}$$

Hence, the conclusion holds. □

As sufficient preparatory works, the above lemmas assist us proving the following discrete energy estimation of the difference scheme (61)–(64). Assume $\{u_i^k \mid 0 \le i \le M,\ 0 \le k \le N\}$ is the solution of the scheme (61)–(64). For simplicity, we firstly define a discrete energy function, i.e.,

$$\begin{aligned} E^k = {} & \frac{\tau^{1-\alpha}}{2\Gamma(2-\alpha)} \sum_{\ell=1}^{k} a_{k-\ell}^{(\alpha)} \Big[\frac{\eta_1^\alpha}{\Gamma(1+\alpha)} \|\delta_t u^{\ell-\frac{1}{2}}\|_l^2 + \frac{\eta_2^\alpha}{\Gamma(1+\alpha)} \|\delta_t u^{\ell-\frac{1}{2}}\|_r^2 \Big] \\ & + \frac{K_{\mathrm{n},1}^2}{6\eta_1} \Big[\|\delta_x u^k\|_l^2 + \frac{1}{\gamma_1 K_{\mathrm{n},1}} (u_0^k)^2 \Big] + \frac{K_{\mathrm{n},2}^2}{6\eta_2} \Big[\|\delta_x u^k\|_r^2 + \frac{1}{\gamma_2 K_{\mathrm{n},2}} (u_M^k)^2 \Big], \quad 1 \le k \le N. \end{aligned} \tag{70}$$

Theorem 2 *The solution* $\{u_i^k \mid 0 \le i \le M,\ 0 \le k \le N\}$ *of the scheme* (61)–(64) *satisfies*

$$\begin{aligned} E^k \le {} & E^0 + \frac{1}{2} \frac{t_k^{1-\alpha}}{\Gamma(2-\alpha)} \Big[\frac{\eta_1^\alpha}{\Gamma(1+\alpha)} \|\psi\|_l^2 + \frac{\eta_2^\alpha}{\Gamma(1+\alpha)} \|\psi\|_r^2 \Big] \\ & + \frac{\tau}{4} \sum_{s=1}^{k} (\|(G)_1^{s-\frac{1}{2}}\|_l^2 + \|(G)_2^{s-\frac{1}{2}}\|_r^2), \quad 1 \le k \le N. \end{aligned} \tag{71}$$

Proof Multiplying (61) by $\frac{h_1}{2}\delta_t u_0^{k-\frac{1}{2}}$ for $i = 0$ and $h_1 \delta_t u_i^{k-\frac{1}{2}}$ for $1 \le i \le m-1$, (62) by $\frac{h_1+h_2}{2}\delta_t u_m^{k-\frac{1}{2}}$, (63) by $h_2 \delta_t u_i^{k-\frac{1}{2}}$ for $m+1 \le i \le M-1$ and $\frac{h_2}{2}\delta_t u_M^{k-\frac{1}{2}}$ for $i = M$, respectively, and then summing up the results, we obtain

$$
\begin{aligned}
&\left(\delta_t u^{k-\frac{1}{2}} + \frac{\eta_1^\alpha}{\Gamma(1+\alpha)}\Delta_\tau^\alpha(\delta_t u^{k-\frac{1}{2}}, \psi), \delta_t u^{k-\frac{1}{2}}\right)_l \\
&\quad + \left(\delta_t u^{k-\frac{1}{2}} + \frac{\eta_2^\alpha}{\Gamma(1+\alpha)}\Delta_\tau^\alpha(\delta_t u^{k-\frac{1}{2}}, \psi), \delta_t u^{k-\frac{1}{2}}\right)_r \\
&= \frac{K_{\mathrm{n},1}^2}{3\eta_1}\Bigg[\frac{h_1}{2}\delta_x^2\Big(u_0^{k-\frac{1}{2}} + \frac{B_1^\beta}{\Gamma(1+\beta)}\delta_\tau^\beta u_0^{k-\frac{1}{2}}\Big)\cdot\delta_t u_0^{k-\frac{1}{2}} \\
&\quad + h_1\sum_{i=1}^{m-1}\delta_x^2\Big(u_i^{k-\frac{1}{2}} + \frac{B_1^\beta}{\Gamma(1+\beta)}\delta_\tau^\beta u_i^{k-\frac{1}{2}}\Big)\cdot\delta_t u_i^{k-\frac{1}{2}} \\
&\quad - \delta_x\Big(u_{m-\frac{1}{2}}^{k-\frac{1}{2}} + \frac{B_1^\beta}{\Gamma(1+\beta)}\delta_\tau^\beta u_{m-\frac{1}{2}}^{k-\frac{1}{2}}\Big)\cdot\delta_t u_m^{k-\frac{1}{2}}\Bigg] \\
&\quad + \frac{K_{\mathrm{n},2}^2}{3\eta_2}\Bigg[\delta_x\Big(u_{m+\frac{1}{2}}^{k-\frac{1}{2}} + \frac{B_2^\beta}{\Gamma(1+\beta)}\delta_\tau^\beta u_{m+\frac{1}{2}}^{k-\frac{1}{2}}\Big)\cdot\delta_t u_m^{k-\frac{1}{2}} \\
&\quad + h_2\sum_{i=m+1}^{M-1}\delta_x^2\Big(u_i^{k-\frac{1}{2}} + \frac{B_2^\beta}{\Gamma(1+\beta)}\delta_\tau^\beta u_i^{k-\frac{1}{2}}\Big)\cdot\delta_t u_i^{k-\frac{1}{2}} \\
&\quad + \frac{h_2}{2}\delta_x^2\Big(u_M^{k-\frac{1}{2}} + \frac{B_2^\beta}{\Gamma(1+\beta)}\delta_\tau^\beta u_M^{k-\frac{1}{2}}\Big)\cdot\delta_t u_M^{k-\frac{1}{2}}\Bigg] \\
&\quad + ((G_1)^{k-\frac{1}{2}}, \delta_t u^{k-\frac{1}{2}})_l + ((G_2)^{k-\frac{1}{2}}, \delta_t u^{k-\frac{1}{2}})_r, \quad 1 \le k \le N. \qquad (72)
\end{aligned}
$$

For the first term on the right hand side of (72), by virtue of the definition (37), the summation by parts and the Cauchy–Schwarz inequality, we have

$$
\begin{aligned}
&\frac{K_{\mathrm{n},1}^2}{3\eta_1}\Bigg[\frac{h_1}{2}\delta_x^2\Big(u_0^{k-\frac{1}{2}} + \frac{B_1^\beta}{\Gamma(1+\beta)}\delta_\tau^\beta u_0^{k-\frac{1}{2}}\Big)\cdot\delta_t u_0^{k-\frac{1}{2}} \\
&\quad + h_1\sum_{i=1}^{m-1}\delta_x^2\Big(u_i^{k-\frac{1}{2}} + \frac{B_1^\beta}{\Gamma(1+\beta)}\delta_\tau^\beta u_i^{k-\frac{1}{2}}\Big)\cdot\delta_t u_i^{k-\frac{1}{2}} \\
&\quad - \delta_x\Big(u_{m-\frac{1}{2}}^{k-\frac{1}{2}} + \frac{B_1^\beta}{\Gamma(1+\beta)}\delta_\tau^\beta u_{m-\frac{1}{2}}^{k-\frac{1}{2}}\Big)\cdot\delta_t u_m^{k-\frac{1}{2}}\Bigg] \\
&= -\frac{K_{\mathrm{n},1}^2}{3\eta_1}\Bigg[\Big(\delta_x\Big(u^{k-\frac{1}{2}} + \frac{B_1^\beta}{\Gamma(1+\beta)}\delta_\tau^\beta u^{k-\frac{1}{2}}\Big), \delta_x(\delta_t u^{k-\frac{1}{2}})\Big)_l \\
&\quad + \frac{1}{\gamma_1 K_{\mathrm{n},1}}\Big(u_0^{k-\frac{1}{2}} + \frac{B_1^\beta}{\Gamma(1+\beta)}\delta_\tau^\beta u_0^{k-\frac{1}{2}}\Big)\cdot\delta_t u_0^{k-\frac{1}{2}}\Bigg] \\
&\le -\frac{1}{\tau}\Bigg[\frac{K_{\mathrm{n},1}^2}{6\eta_1}\Big(\|\delta_x u^k\|_l^2 + \frac{1}{\gamma_1 K_{\mathrm{n},1}}(u_0^k)^2\Big) - \frac{K_{\mathrm{n},1}^2}{6\eta_1}\Big(\|\delta_x u^{k-1}\|_l^2 + \frac{1}{\gamma_1 K_{\mathrm{n},1}}(u_0^{k-1})^2\Big)\Bigg] \\
&\quad - \frac{K_{\mathrm{n},1}^2}{3\eta_1}\frac{B_1^\beta}{\Gamma(1+\beta)}\Bigg[\big(\delta_\tau^\beta(\delta_x u^{k-\frac{1}{2}}), \delta_t(\delta_x u^{k-\frac{1}{2}})\big)_l + \frac{1}{\gamma_1 K_{\mathrm{n},1}}(\delta_\tau^\beta u_0^{k-\frac{1}{2}})\cdot\delta_t u_0^{k-\frac{1}{2}}\Bigg]. \qquad (73)
\end{aligned}
$$

Similarly, for the second term on the right hand side of (72), we get

$$\begin{aligned}
&\frac{K_{\mathrm{n},2}^2}{3\eta_2}\Big[\delta_x\Big(u_{m+\frac{1}{2}}^{k-\frac{1}{2}}+\frac{B_2^\beta}{\Gamma(1+\beta)}\delta_\tau^\beta u_{m+\frac{1}{2}}^{k-\frac{1}{2}}\Big)\cdot\delta_t u_m^{k-\frac{1}{2}}\\
&\quad+h_2\sum_{i=m+1}^{M-1}\delta_x^2\Big(u_i^{k-\frac{1}{2}}+\frac{B_2^\beta}{\Gamma(1+\beta)}\delta_\tau^\beta u_i^{k-\frac{1}{2}}\Big)\cdot\delta_t u_i^{k-\frac{1}{2}}\\
&\quad+\frac{h_2}{2}\delta_x^2\Big(u_M^{k-\frac{1}{2}}+\frac{B_2^\beta}{\Gamma(1+\beta)}\delta_\tau^\beta u_M^{k-\frac{1}{2}}\Big)\cdot\delta_t u_M^{k-\frac{1}{2}}\Big]\\
&\le-\frac{1}{\tau}\Big[\frac{K_{\mathrm{n},2}^2}{6\eta_2}\Big(\|\delta_x u^k\|_r^2+\frac{1}{\gamma_2 K_{\mathrm{n},2}}(u_M^k)^2\Big)-\frac{K_{\mathrm{n},2}^2}{6\eta_2}\Big(\|\delta_x u^{k-1}\|_r^2+\frac{1}{\gamma_2 K_{\mathrm{n},2}}(u_M^{k-1})^2\Big)\Big]\\
&\quad-\frac{K_{\mathrm{n},2}^2}{3\eta_2}\frac{B_2^\beta}{\Gamma(1+\beta)}\Big[\big(\delta_\tau^\beta(\delta_x u^{k-\frac{1}{2}}),\delta_t(\delta_x u^{k-\frac{1}{2}})\big)_r+\frac{1}{\gamma_2 K_{\mathrm{n},2}}(\delta_\tau^\beta u_M^{k-\frac{1}{2}})\cdot\delta_t u_M^{k-\frac{1}{2}}\Big].
\end{aligned}\tag{74}$$

Using the Cauchy–Schwarz inequality again for the last two terms on the right hand side of (72), we have

$$\begin{aligned}
&((G_1)^{k-\frac{1}{2}},\delta_t u^{k-\frac{1}{2}})_l+((G_2)^{k-\frac{1}{2}},\delta_t u^{k-\frac{1}{2}})_r\le\|\delta_t u^{k-\frac{1}{2}}\|_l^2+\|\delta_t u^{k-\frac{1}{2}}\|_r^2\\
&\quad+\frac{1}{4}(\|(G)_1^{k-\frac{1}{2}}\|_l^2+\|(G)_2^{k-\frac{1}{2}}\|_r^2).
\end{aligned}\tag{75}$$

Inserting (73)–(75) into (72), replacing the superscript k with s and summing up s from 1 to k on both sides of the result, then using Lemma 6 with $\epsilon=\frac{1}{2}$ and Lemma 7, we get the conclusion. □

From Lemma 8, we have an estimate

$$\begin{aligned}
&\frac{K_{\mathrm{n},1}^2}{6\eta_1}\Big[\|\delta_x u^k\|_l^2+\frac{1}{\gamma_1 K_{\mathrm{n},1}}(u_0^k)^2\Big]+\frac{K_{\mathrm{n},2}^2}{6\eta_2}\Big[\|\delta_x u^k\|_r^2+\frac{1}{\gamma_2 K_{\mathrm{n},2}}(u_M^k)^2\Big]\\
&\quad=c_1\Big[(1+\frac{l_x}{\gamma_1 K_{\mathrm{n},1}})(u_0^k)^2+(1+\frac{\gamma_1 K_{\mathrm{n},1}}{l_x})l_x\|\delta_x u^k\|_l^2\Big]\\
&\qquad+c_2\Big[(1+\frac{L_x-l_x}{\gamma_2 K_{\mathrm{n},2}})(u_M^k)^2+(1+\frac{\gamma_2 K_{\mathrm{n},2}}{L_x-l_x})(L_x-l_x)\|\delta_x u^k\|_r^2\Big]\\
&\quad\ge c_1\|u^k\|_{l,\infty}^2+c_2\|u^k\|_{r,\infty}^2,
\end{aligned}\tag{76}$$

where $c_1=\frac{K_{\mathrm{n},1}^2}{6\eta_1(\gamma_1 K_{\mathrm{n},1}+l_x)}$ and $c_2=\frac{K_{\mathrm{n},2}^2}{6\eta_2(\gamma_2 K_{\mathrm{n},2}+L_x-l_x)}$.

Theorem 2 and the estimate (76) indicate the following stability conclusion.

Corollary 1 (Stability) *The scheme (61)–(64) is unconditionally stable with respect to the initial values and the source terms, i.e.,*

$$\begin{aligned}
c_1\|u^k\|_{l,\infty}^2+c_2\|u^k\|_{r,\infty}^2\le&\frac{K_{\mathrm{n},1}^2}{6\eta_1}\Big[\|\delta_x u^0\|_l^2+\frac{1}{\gamma_1 K_{\mathrm{n},1}}(u_0^0)^2\Big]\\
&+\frac{K_{\mathrm{n},2}^2}{6\eta_2}\Big[\|\delta_x u^0\|_r^2+\frac{1}{\gamma_2 K_{\mathrm{n},2}}(u_M^0)^2\Big]\\
&+\frac{1}{2}\frac{t_k^{1-\alpha}}{\Gamma(2-\alpha)}\Big[\frac{\eta_1^\alpha}{\Gamma(1+\alpha)}\|\psi\|_l^2+\frac{\eta_2^\alpha}{\Gamma(1+\alpha)}\|\psi\|_r^2\Big]\\
&+\frac{\tau}{4}\sum_{s=1}^{k}(\|(G)_1^{s-\frac{1}{2}}\|_l^2+\|(G)_2^{s-\frac{1}{2}}\|_r^2),\quad 1\le k\le N.
\end{aligned}$$

Assume $u(x,t)$ is the solution of (10)–(16) and $\{u_i^k \mid 0 \le i \le M,\ 0 \le k \le N\}$ is the solution of the scheme (61)–(64). We denote the errors

$$e_i^n = u(x_i, t_n) - u_i^n, \quad 0 \le i \le M, \quad 0 \le k \le N. \tag{77}$$

Subtracting (61)–(64) from (50)– (52) and (60), respectively, we can easily get the following error equations

$$\begin{aligned}
&\delta_t e_i^{k-\frac{1}{2}} + \frac{\eta_1^\alpha}{\Gamma(1+\alpha)} \Delta_\tau^\alpha \big(\delta_t e_i^{k-\frac{1}{2}}, 0\big) = \frac{K_{\mathrm{n},1}^2}{3\eta_1} \delta_x^2 \Big(e_i^{k-\frac{1}{2}} + \frac{B_1^\beta}{\Gamma(1+\beta)} \delta_\tau^\beta e_i^{k-\frac{1}{2}} \Big) \\
&\quad + (R^t)_i^{k-\frac{1}{2}} + (R^x)_i^{k-\frac{1}{2}}, \\
&\quad i \in \omega_l \backslash \{m\}, \quad 1 \le k \le N, \qquad (78) \\
&\frac{h_1}{h_1+h_2} \Big(\delta_t e_m^{k-\frac{1}{2}} + \frac{\eta_1^\alpha}{\Gamma(1+\alpha)} \Delta_\tau^\alpha \big(\delta_t e_m^{k-\frac{1}{2}}, 0\big) \Big) \\
&\quad + \frac{h_2}{h_1+h_2} \Big(\delta_t e_m^{k-\frac{1}{2}} + \frac{\eta_2^\alpha}{\Gamma(1+\alpha)} \Delta_\tau^\alpha \big(\delta_t e_m^{k-\frac{1}{2}}, 0\big) \Big) \\
&= \frac{2}{3(h_1+h_2)} \Bigg[\frac{K_{\mathrm{n},2}^2}{\eta_2} \delta_x \Big(e_{m+\frac{1}{2}}^{k-\frac{1}{2}} + \frac{B_2^\beta}{\Gamma(1+\beta)} \delta_\tau^\beta e_{m+\frac{1}{2}}^{k-\frac{1}{2}} \Big) \\
&\quad - \frac{K_{\mathrm{n},1}^2}{\eta_1} \delta_x \Big(e_{m-\frac{1}{2}}^{k-\frac{1}{2}} + \frac{B_1^\beta}{\Gamma(1+\beta)} \delta_\tau^\beta e_{m-\frac{1}{2}}^{k-\frac{1}{2}} \Big) \Bigg] \\
&\quad + \frac{h_1}{h_1+h_2} \Big((R^t)_m^{k-\frac{1}{2}} + (R^x)_m^{k-\frac{1}{2}} \Big) \\
&\quad + \frac{h_2}{h_1+h_2} \Big((S^t)_m^{k-\frac{1}{2}} + (S^x)_m^{k-\frac{1}{2}} \Big), \quad 1 \le k \le N, \qquad (79) \\
&\delta_t e_i^{k-\frac{1}{2}} + \frac{\eta_2^\alpha}{\Gamma(1+\alpha)} \Delta_\tau^\alpha \big(\delta_t e_i^{k-\frac{1}{2}}, 0\big) = \frac{K_{\mathrm{n},2}^2}{3\eta_2} \delta_x^2 \Big(e_i^{k-\frac{1}{2}} + \frac{B_2^\beta}{\Gamma(1+\beta)} \delta_\tau^\beta e_i^{k-\frac{1}{2}} \Big) \\
&\quad + (S^t)_i^{k-\frac{1}{2}} + (S^x)_i^{k-\frac{1}{2}}, \\
&\quad i \in \omega_r \backslash \{m\}, \quad 1 \le k \le N, \qquad (80) \\
&e_i^0 = 0, \quad i \in \omega_l \cup \omega_r. \qquad (81)
\end{aligned}$$

An immediate application of Theorem 2 deduces that the convergence order in space of the scheme (61)–(64) is $O(h_1^{3/2} + h_2^{3/2})$. In fact, the spatial convergence accuracy of the scheme in this paper is higher than the order of $3/2$, which can be confirmed in the subsequent simulations. In the next theorem, we will give the theoretical analysis of convergence accuracies. We omit some processes which are similar to those in Theorem 2.

Theorem 3 (Convergence) *The finite difference scheme* (61)–(64) *for the fractional DPL model* (10)–(16) *admits*

$$\|e^k\|_\infty \le c_3 (\tau^{\min\{2-\alpha, 2-\beta\}} + h_1^2 + h_2^2), \quad 0 \le k \le N, \tag{82}$$

where c_3 is a positive constant independent of τ, h_1 and h_2.

Proof Multiplying (78) by $\frac{h_1}{2} \delta_t e_0^{k-\frac{1}{2}}$ for $i = 0$ and $h_1 \delta_t e_i^{k-\frac{1}{2}}$ for $1 \le i \le m-1$, (79) by $\frac{h_1+h_2}{2} \delta_t e_m^{k-\frac{1}{2}}$, (80) by $h_2 \delta_t e_i^{k-\frac{1}{2}}$ for $m+1 \le i \le M-1$ and $\frac{h_2}{2} \delta_t e_M^{k-\frac{1}{2}}$ for $i = M$, respectively, and then summing up the results, we obtain

$$
\begin{aligned}
&\left(\delta_t e^{k-\frac{1}{2}} + \frac{\eta_1^\alpha}{\Gamma(1+\alpha)}\Delta_\tau^\alpha(\delta_t e^{k-\frac{1}{2}},0),\delta_t e^{k-\frac{1}{2}}\right)_l \\
&\quad + \left(\delta_t e^{k-\frac{1}{2}} + \frac{\eta_2^\alpha}{\Gamma(1+\alpha)}\Delta_\tau^\alpha(\delta_t e^{k-\frac{1}{2}},0),\delta_t e^{k-\frac{1}{2}}\right)_r \\
&= \frac{K_{\mathrm{n},1}^2}{3\eta_1}\left[\frac{h_1}{2}\delta_x^2\left(e_0^{k-\frac{1}{2}} + \frac{B_1^\beta}{\Gamma(1+\beta)}\delta_\tau^\beta e_0^{k-\frac{1}{2}}\right)\cdot\delta_t e_0^{k-\frac{1}{2}}\right. \\
&\quad + h_1\sum_{i=1}^{m-1}\delta_x^2\left(e_i^{k-\frac{1}{2}} + \frac{B_1^\beta}{\Gamma(1+\beta)}\delta_\tau^\beta e_i^{k-\frac{1}{2}}\right)\cdot\delta_t e_i^{k-\frac{1}{2}} \\
&\quad \left. - \delta_x\left(e_{m-\frac{1}{2}}^{k-\frac{1}{2}} + \frac{B_1^\beta}{\Gamma(1+\beta)}\delta_\tau^\beta e_{m-\frac{1}{2}}^{k-\frac{1}{2}}\right)\cdot\delta_t e_m^{k-\frac{1}{2}}\right] \\
&\quad + \frac{K_{\mathrm{n},2}^2}{3\eta_2}\left[\delta_x\left(e_{m+\frac{1}{2}}^{k-\frac{1}{2}} + \frac{B_2^\beta}{\Gamma(1+\beta)}\delta_\tau^\beta e_{m+\frac{1}{2}}^{k-\frac{1}{2}}\right)\cdot\delta_t e_m^{k-\frac{1}{2}}\right. \\
&\quad + h_2\sum_{i=m+1}^{M-1}\delta_x^2\left(e_i^{k-\frac{1}{2}} + \frac{B_2^\beta}{\Gamma(1+\beta)}\delta_\tau^\beta e_i^{k-\frac{1}{2}}\right)\cdot\delta_t e_i^{k-\frac{1}{2}} \\
&\quad \left. + \frac{h_2}{2}\delta_x^2\left(e_M^{k-\frac{1}{2}} + \frac{B_2^\beta}{\Gamma(1+\beta)}\delta_\tau^\beta e_M^{k-\frac{1}{2}}\right)\cdot\delta_t e_M^{k-\frac{1}{2}}\right] \\
&\quad + ((R^t)^{k-\frac{1}{2}} + (R^x)^{k-\frac{1}{2}},\delta_t e^{k-\frac{1}{2}})_l + ((S^t)^{k-\frac{1}{2}} + (S^x)^{k-\frac{1}{2}},\delta_t e^{k-\frac{1}{2}})_r, \quad 1\le k\le N.
\end{aligned}
\tag{83}
$$

According to (73) and (74), for the first two terms on the right hand side of (83), we have

$$
\begin{aligned}
&\frac{K_{\mathrm{n},1}^2}{3\eta_1}\left[\frac{h_1}{2}\delta_x^2\left(e_0^{k-\frac{1}{2}} + \frac{B_1^\beta}{\Gamma(1+\beta)}\delta_\tau^\beta e_0^{k-\frac{1}{2}}\right)\delta_t e_0^{k-\frac{1}{2}}\right. \\
&\quad + h_1\sum_{i=1}^{m-1}\delta_x^2\left(e_i^{k-\frac{1}{2}} + \frac{B_1^\beta}{\Gamma(1+\beta)}\delta_\tau^\beta e_i^{k-\frac{1}{2}}\right)\cdot\delta_t e_i^{k-\frac{1}{2}} \\
&\quad \left. - \delta_x\left(e_{m-\frac{1}{2}}^{k-\frac{1}{2}} + \frac{B_1^\beta}{\Gamma(1+\beta)}\delta_\tau^\beta e_{m-\frac{1}{2}}^{k-\frac{1}{2}}\right)\cdot\delta_t e_m^{k-\frac{1}{2}}\right] \\
&\le -\frac{1}{\tau}\left[\frac{K_{\mathrm{n},1}^2}{6\eta_1}\left(\|\delta_x e^k\|_l^2 + \frac{1}{\gamma_1 K_{\mathrm{n},1}}(e_0^k)^2\right) - \frac{K_{\mathrm{n},1}^2}{6\eta_1}\left(\|\delta_x e^{k-1}\|_l^2 + \frac{1}{\gamma_1 K_{\mathrm{n},1}}(e_0^{k-1})^2\right)\right] \\
&\quad - \frac{K_{\mathrm{n},1}^2}{3\eta_1}\frac{B_1^\beta}{\Gamma(1+\beta)}\left[\left(\delta_\tau^\beta(\delta_x e^{k-\frac{1}{2}}),\delta_t(\delta_x e^{k-\frac{1}{2}})\right)_l + \frac{1}{\gamma_1 K_{\mathrm{n},1}}(\delta_\tau^\beta e_0^{k-\frac{1}{2}})\cdot\delta_t e_0^{k-\frac{1}{2}}\right],
\end{aligned}
\tag{84}
$$

and

$$
\begin{aligned}
&\frac{K_{\mathrm{n},2}^2}{3\eta_2}\left[\delta_x\left(e_{m+\frac{1}{2}}^{k-\frac{1}{2}} + \frac{B_2^\beta}{\Gamma(1+\beta)}\delta_\tau^\beta e_{m+\frac{1}{2}}^{k-\frac{1}{2}}\right)\cdot\delta_t e_m^{k-\frac{1}{2}}\right. \\
&\quad \left. + h_2\sum_{i=m+1}^{M-1}\delta_x^2\left(e_i^{k-\frac{1}{2}} + \frac{B_2^\beta}{\Gamma(1+\beta)}\delta_\tau^\beta e_i^{k-\frac{1}{2}}\right)\delta_t e_i^{k-\frac{1}{2}}\right.
\end{aligned}
$$

Table 1 Maximum errors and spatial convergence orders for Example 1 ($\tau = \frac{1}{500}$)

(α, β)	h	$K_{n,1} = K_{n,2} = 0.1$		$K_{n,1} = K_{n,2} = 1$		$K_{n,1} = K_{n,2} = 10$	
		$\text{Error}_\tau(h)$	$\text{Order}_\tau(h)$	$\text{Error}_\tau(h)$	$\text{Order}_\tau(h)$	$\text{Error}_\tau(h)$	$\text{Order}_\tau(h)$
(0.9,0.1)	1/80	2.995e−04		6.920e−06		4.886e−07	
	1/160	7.438e−05	2.0	1.729e−06	2.0	1.222e−07	2.0
	1/320	1.858e−05	2.0	4.323e−07	2.0	3.054e−08	2.0
(0.5,0.5)	1/80	2.679e−04		6.987e−06		3.790e−07	
	1/160	6.710e−05	2.0	1.747e−06	2.0	9.474e−08	2.0
	1/320	1.678e−05	2.0	4.367e−07	2.0	2.368e−08	2.0
(0.1,0.9)	1/80	2.757e−04		7.217e−06		3.895e−07	
	1/160	6.940e−05	2.0	1.804e−06	2.0	9.737e−08	2.0
	1/320	1.738e−05	2.0	4.511e−07	2.0	2.434e−08	2.0

Table 2 Maximum errors and temporal convergence orders for Example 1 ($h = \frac{1}{100}$)

(α, β)	τ	$K_{n,1} = K_{n,2} = 0.1$		$K_{n,1} = K_{n,2} = 1$		$K_{n,1} = K_{n,2} = 10$	
		$\text{Error}_h(\tau)$	$\text{Order}_h(\tau)$	$\text{Error}_h(\tau)$	$\text{Order}_h(\tau)$	$\text{Error}_h(\tau)$	$\text{Order}_h(\tau)$
(0.9,0.1)	1/200	1.828e−04		8.653e−05		7.874e−05	
	1/400	8.542e−05	1.1	4.062e−05	1.1	3.751e−05	1.1
	1/800	3.989e−05	1.1	1.900e−05	1.1	1.771e−05	1.1
(0.5,0.5)	1/200	6.492e−06		1.605e−06		5.333e−07	
	1/400	2.312e−06	1.5	5.728e−07	1.5	1.951e−07	1.5
	1/800	8.214e−07	1.5	2.039e−07	1.5	7.071e−08	1.5
(0.1,0.3)	1/200	1.516e−07		3.444e−07		1.616e−07	
	1/400	4.697e−08	1.7	1.088e−07	1.7	4.535e−08	1.7
	1/800	1.458e−08	1.7	3.430e−08	1.7	1.329e−08	1.7

Table 3 Properties of gold and chromium

Property	Gold	Chromium
τ_q (ps)	8.5	0.136
τ_T (ps)	90	7.86
κ (W/m K)	315	94
c_ρ (J/kg K)	129	449
ρ (kg/m^3)	19,300	7160

Table 4 Maximum errors and spatial convergence orders for Example 2 ($\tau = \frac{1}{500}$)

(α, β)	h	$G = 0.1$		$G = 1$		$G = 10$	
		$\text{Error}_\tau(h)$	$\text{Order}_\tau(h)$	$\text{Error}_\tau(h)$	$\text{Order}_\tau(h)$	$\text{Error}_\tau(h)$	$\text{Order}_\tau(h)$
(0.7,0.3)	$L_x/20$	2.452e−04		2.448e−04		2.448e−04	
	$L_x/40$	6.129e−05	2.0	6.121e−05	2.0	6.120e−05	2.0
	$L_x/80$	1.532e−05	2.0	1.530e−05	2.0	1.530e−05	2.0

Table 5 Maximum errors and temporal convergence orders for Example 2 ($h = \frac{L_x}{200}$)

(α, β)	τ	$G = 0.1$		$G = 1$		$G = 10$	
		$\text{Error}_h(\tau)$	$\text{Order}_h(\tau)$	$\text{Error}_h(\tau)$	$\text{Order}_h(\tau)$	$\text{Error}_h(\tau)$	$\text{Order}_h(\tau)$
(0.7,0.3)	1/500	2.909e−06		1.987e−06		1.894e−06	
	1/1000	1.173e−06	1.3	7.935e−07	1.3	7.533e−07	1.3
	1/2000	4.693e−07	1.3	3.175e−07	1.3	3.049e−07	1.3
	1/4000	1.916e−07	1.3	1.285e−07	1.3	1.224e−07	1.3

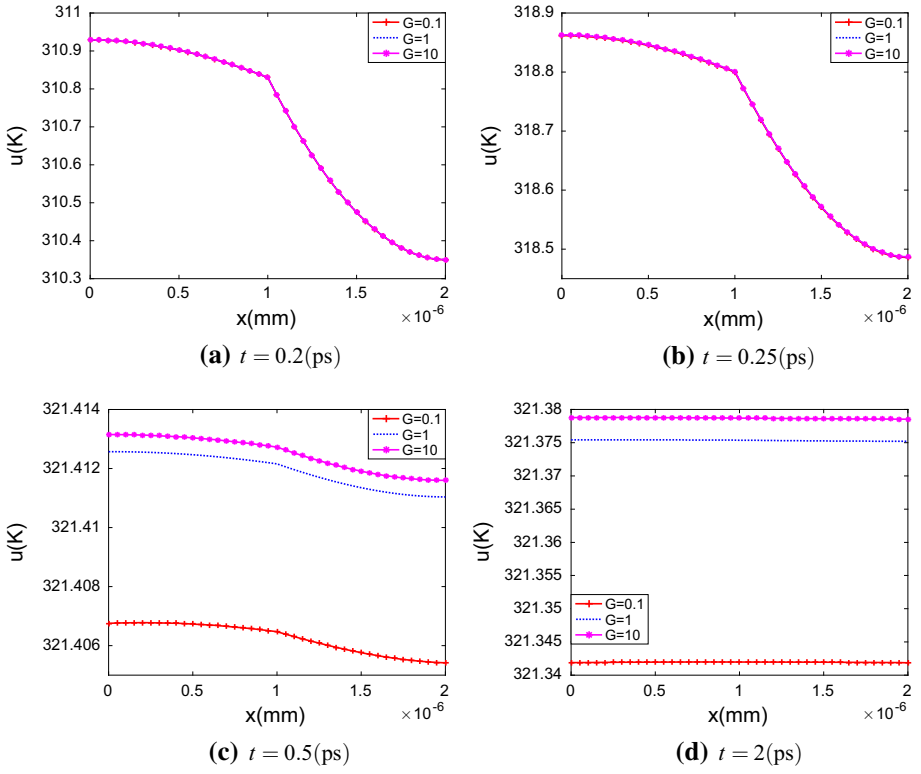

(a) $t = 0.2$(ps) **(b)** $t = 0.25$(ps)

(c) $t = 0.5$(ps) **(d)** $t = 2$(ps)

Fig. 2 Temperature profiles at $t = 0.2$ (ps), 0.25 (ps), 0.5 (ps), 2 (ps) for $(\alpha, \beta) = (0.1, 0.1)$

$$
\begin{aligned}
&+ \frac{h_2}{2}\delta_x^2\Big(e_M^{k-\frac{1}{2}} + \frac{B_2^\beta}{\Gamma(1+\beta)}\delta_\tau^\beta e_M^{k-\frac{1}{2}}\Big)\cdot\delta_t e_M^{k-\frac{1}{2}}\Big] \\
&\le -\frac{1}{\tau}\Big[\frac{K_{\mathrm{n},2}^2}{6\eta_2}\Big(\|\delta_x e^k\|_r^2 + \frac{1}{\gamma_2 K_{\mathrm{n},2}}(e_M^k)^2\Big) - \frac{K_{\mathrm{n},2}^2}{6\eta_2}\Big(\|\delta_x e^{k-1}\|_r^2 + \frac{1}{\gamma_2 K_{\mathrm{n},2}}(e_M^{k-1})^2\Big)\Big] \\
&- \frac{K_{\mathrm{n},2}^2}{3\eta_2}\frac{B_2^\beta}{\Gamma(1+\beta)}\Big[\big(\delta_\tau^\beta(\delta_x e^{k-\frac{1}{2}}), \delta_t(\delta_x e^{k-\frac{1}{2}})\big)_r + \frac{1}{\gamma_2 K_{\mathrm{n},2}}(\delta_\tau^\beta e_M^{k-\frac{1}{2}})\cdot\delta_t e_M^{k-\frac{1}{2}}\Big]. \quad (85)
\end{aligned}
$$

Denote

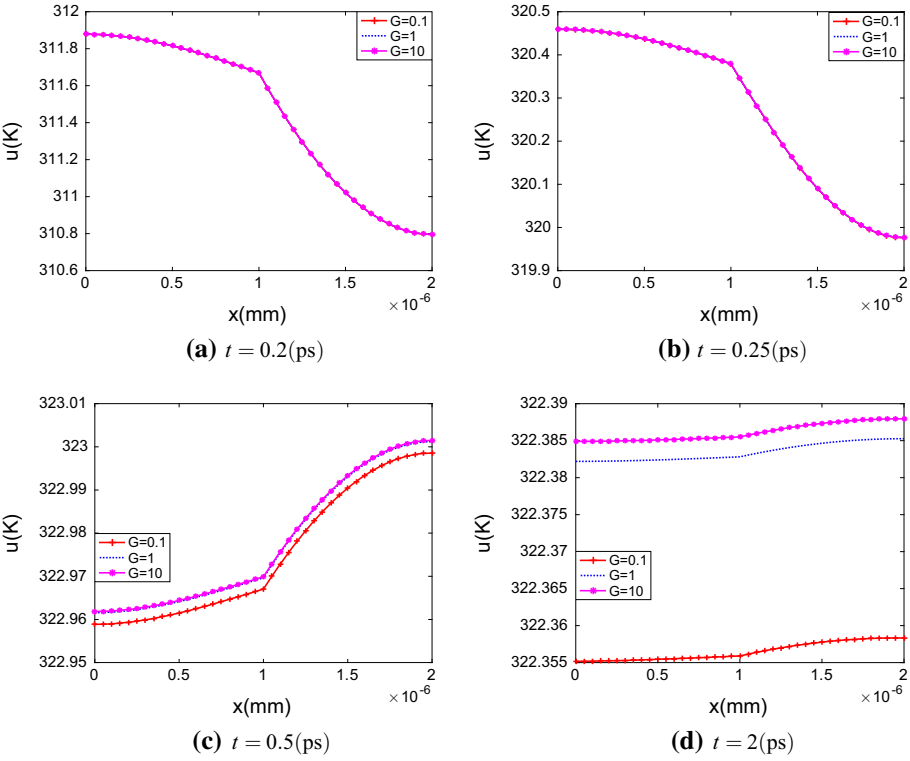

(a) $t = 0.2(\text{ps})$ **(b)** $t = 0.25(\text{ps})$

(c) $t = 0.5(\text{ps})$ **(d)** $t = 2(\text{ps})$

Fig. 3 Temperature profiles at $t = 0.2$ (ps), 0.25 (ps), 0.5 (ps), 2 (ps) for $(\alpha, \beta) = (0.5, 0.1)$

$$F^k = \frac{\tau^{1-\alpha}}{2\Gamma(2-\alpha)} \sum_{\ell=1}^{k} a_{k-\ell}^{(\alpha)} \left[\frac{\eta_1^\alpha}{\Gamma(1+\alpha)} \|\delta_t e^{\ell-\frac{1}{2}}\|_l^2 + \frac{\eta_2^\alpha}{\Gamma(1+\alpha)} \|\delta_t e^{\ell-\frac{1}{2}}\|_r^2 \right]$$
$$+ \frac{K_{\mathrm{n},1}^2}{6\eta_1} \left[\|\delta_x e^k\|_l^2 + \frac{1}{\gamma_1 K_{\mathrm{n},1}} (e_0^k)^2 \right] + \frac{K_{\mathrm{n},2}^2}{6\eta_2} \left[\|\delta_x e^k\|_r^2 + \frac{1}{\gamma_2 K_{\mathrm{n},2}} (e_M^k)^2 \right], \quad 1 \le k \le N. \tag{86}$$

Inserting (84) and (85) into (83), replacing the superscript k with s and summing up s from 1 to k on both sides of the result, then using Lemma 6 with $\epsilon = \frac{1}{2}$ and Lemma 7, we get

$$F^k + \tau \sum_{s=1}^{k} \left(\|\delta_t e^{s-\frac{1}{2}}\|_l^2 + \|\delta_t e^{s-\frac{1}{2}}\|_r^2 \right)$$
$$\le \tau \sum_{s=1}^{k} \left[\left((R^t)^{s-\frac{1}{2}} + (R^x)^{s-\frac{1}{2}}, \delta_t e^{s-\frac{1}{2}} \right)_l + \left((S^t)^{s-\frac{1}{2}} + (S^x)^{s-\frac{1}{2}}, \delta_t e^{s-\frac{1}{2}} \right)_r \right]$$
$$= \tau \sum_{s=1}^{k} \left((R^t)^{s-\frac{1}{2}}, \delta_t e^{s-\frac{1}{2}} \right)_l + \tau \sum_{s=1}^{k} h_1 \sum_{i=1}^{m-1} (R^x)_i^{s-\frac{1}{2}} \cdot \delta_t e_i^{s-\frac{1}{2}}$$

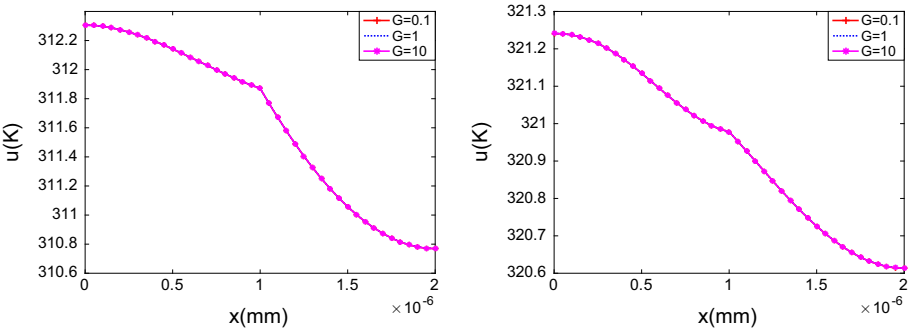

(a) $t = 0.2(\text{ps})$ **(b)** $t = 0.25(\text{ps})$

(c) $t = 0.5(\text{ps})$ **(d)** $t = 2(\text{ps})$

Fig. 4 Temperature profiles at $t = 0.2$ (ps), 0.25 (ps), 0.5 (ps), 2 (ps) for $(\alpha, \beta) = (0.9, 0.1)$

$$
\begin{aligned}
&+\tau\sum_{s=1}^{k}\frac{h_1}{2}\sum_{i=0,m}(R^x)_i^{s-\frac{1}{2}}\cdot\delta_t e_i^{s-\frac{1}{2}}\\
&+\tau\sum_{s=1}^{k}\left((S^t)^{s-\frac{1}{2}},\delta_t e^{s-\frac{1}{2}}\right)_r+\tau\sum_{s=1}^{k}h_2\sum_{i=m+1}^{M-1}(S^x)_i^{s-\frac{1}{2}}\cdot\delta_t e_i^{s-\frac{1}{2}}\\
&+\tau\sum_{s=1}^{k}\frac{h_2}{2}\sum_{i=m,M}(S^x)_i^{s-\frac{1}{2}}\cdot\delta_t e_i^{s-\frac{1}{2}}.
\end{aligned}
\tag{87}
$$

For the first two terms on the right hand side of (87), by using the Cauchy–Schwarz inequality, we have

$$
\begin{aligned}
&\tau\sum_{s=1}^{k}\left((R^t)^{s-\frac{1}{2}},\delta_t e^{s-\frac{1}{2}}\right)_l+\tau\sum_{s=1}^{k}h_1\sum_{i=1}^{m-1}(R^x)_i^{s-\frac{1}{2}}\cdot\delta_t e_i^{s-\frac{1}{2}}\\
&\quad\le\tau\sum_{s=1}^{k}\|\delta_t e^{s-\frac{1}{2}}\|_l^2+\frac{\tau}{2}\sum_{s=1}^{k}\left[\|(R^t)^{s-\frac{1}{2}}\|_l^2+h_1\sum_{i=1}^{m-1}\left((R^x)_i^{s-\frac{1}{2}}\right)^2\right].
\end{aligned}
\tag{88}
$$

Similarly, applying the Cauchy–Schwarz inequality for the fourth term and fifth term on the right hand side of (87) leads to

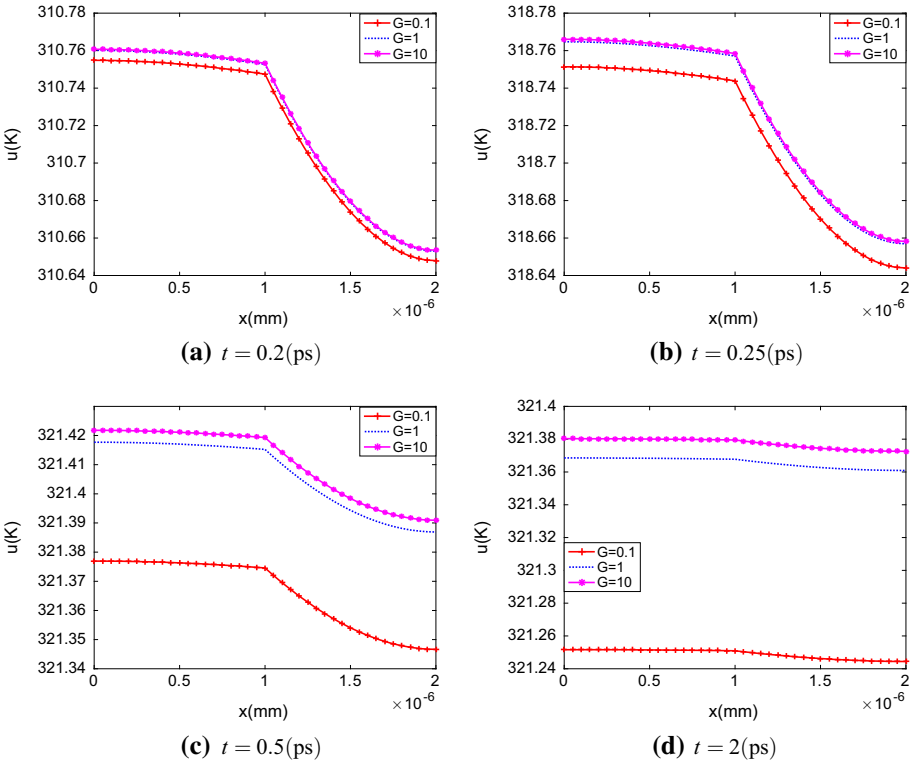

(a) $t = 0.2$(ps) **(b)** $t = 0.25$(ps)

(c) $t = 0.5$(ps) **(d)** $t = 2$(ps)

Fig. 5 Temperature profiles at $t = 0.2$ (ps), 0.25 (ps), 0.5 (ps), 2 (ps) for $(\alpha, \beta) = (0.1, 0.5)$

$$\tau \sum_{s=1}^{k} \left((S^t)^{s-\frac{1}{2}}, \delta_t e^{s-\frac{1}{2}} \right)_r + \tau \sum_{s=1}^{k} h_1 \sum_{i=1}^{m-1} (S^x)_i^{s-\frac{1}{2}} \cdot \delta_t e_i^{s-\frac{1}{2}}$$
$$\leq \tau \sum_{s=1}^{k} \| \delta_t e^{s-\frac{1}{2}} \|_r^2 + \frac{\tau}{2} \sum_{s=1}^{k} \left[\| (S^t)^{s-\frac{1}{2}} \|_r^2 + h_2 \sum_{i=m+1}^{M-1} \left((S^x)_i^{s-\frac{1}{2}} \right)^2 \right]. \tag{89}$$

To provide convergence order in space, we adopt a strategy different from (88), specifically,

$$\frac{\tau}{2} \sum_{s=1}^{k} h_1 \sum_{i=0,m} (R^x)_i^{s-\frac{1}{2}} \cdot \delta_t e_i^{s-\frac{1}{2}}$$
$$= \frac{h_1}{2} \sum_{i=0,m} \left[(R^x)_i^{k-\frac{1}{2}} \cdot e_i^k - \tau \sum_{s=1}^{k-1} \frac{(R^x)_i^{s+\frac{1}{2}} - (R^x)_i^{s-\frac{1}{2}}}{\tau} \cdot e_i^s \right]$$
$$\leq \frac{c_1}{2} \left[\| e^k \|_{l,\infty}^2 + \tau \sum_{s=1}^{k-1} \| e^s \|_{l,\infty}^2 \right] + \frac{h_1^2}{4c_1} \sum_{i=0,m} \left[|(R^x)_i^{k-\frac{1}{2}}|^2 \right.$$
$$\left. + \tau \sum_{s=1}^{k-1} \left| \frac{(R^x)_i^{s+\frac{1}{2}} - (R^x)_i^{s-\frac{1}{2}}}{\tau} \right|^2 \right], \tag{90}$$

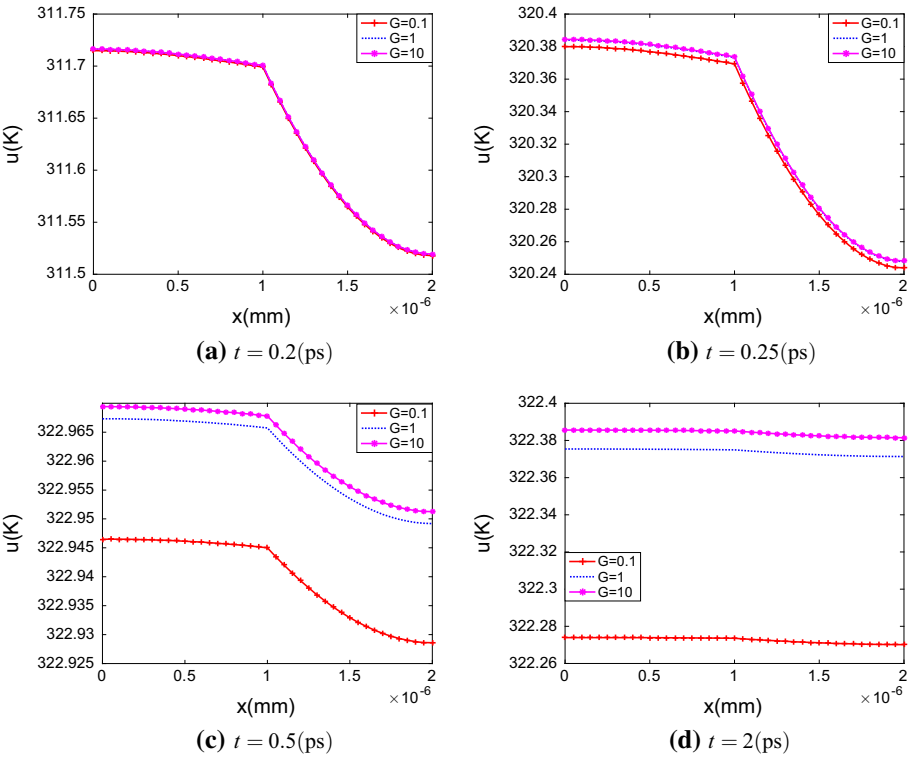

(a) $t = 0.2$(ps) **(b)** $t = 0.25$(ps)

(c) $t = 0.5$(ps) **(d)** $t = 2$(ps)

Fig. 6 Temperature profiles at $t = 0.2$ (ps), 0.25 (ps), 0.5 (ps), 2 (ps) for $(\alpha, \beta) = (0.5, 0.5)$

and

$$\begin{aligned}
&\frac{\tau}{2}\sum_{s=1}^{k} h_2 \sum_{i=m,M} (S^x)_i^{s-\frac{1}{2}} \cdot \delta_t e_i^{s-\frac{1}{2}} \\
&= \frac{h_2}{2}\sum_{i=m,M}\left[(S^x)_i^{k-\frac{1}{2}} \cdot e_i^k - \tau\sum_{s=1}^{k-1}\frac{(S^x)_i^{s+\frac{1}{2}} - (S^x)_i^{s-\frac{1}{2}}}{\tau}\cdot e_i^s\right] \\
&\le \frac{c_2}{2}\left[\|e^k\|_{r,\infty}^2 + \tau\sum_{s=1}^{k-1}\|e^s\|_{r,\infty}^2\right] + \frac{h_2^2}{4c_2}\sum_{i=m,M}\left[|(S^x)_i^{k-\frac{1}{2}}|^2\right. \\
&\quad \left. + \tau\sum_{s=1}^{k-1}\left|\frac{(S^x)_i^{s+\frac{1}{2}} - (S^x)_i^{s-\frac{1}{2}}}{\tau}\right|^2\right],
\end{aligned} \tag{91}$$

where c_1 and c_2 are defined in (76). Here, we have used the fact $e_i^0 = 0,\ i \in \omega_l \cup \omega_r$.

Inserting the above estimations (88)–(91) into (87), and noticing the truncation errors (53)–(59) and $F^k \ge c_1\|e^k\|_{l,\infty}^2 + c_2\|e^k\|_{r,\infty}^2$, we have

$$\begin{aligned}
c_1\|e^k\|_{l,\infty}^2 + c_2\|e^k\|_{r,\infty}^2 &\le \tau\sum_{s=1}^{k-1}\left[c_1\|e^s\|_{l,\infty}^2 + c_2\|e^s\|_{r,\infty}^2\right] \\
&\quad + c_4(\tau^{\min\{2-\alpha,2-\beta\}} + h_1^2 + h_2^2)^2, \quad 1 \le k \le N,
\end{aligned}$$

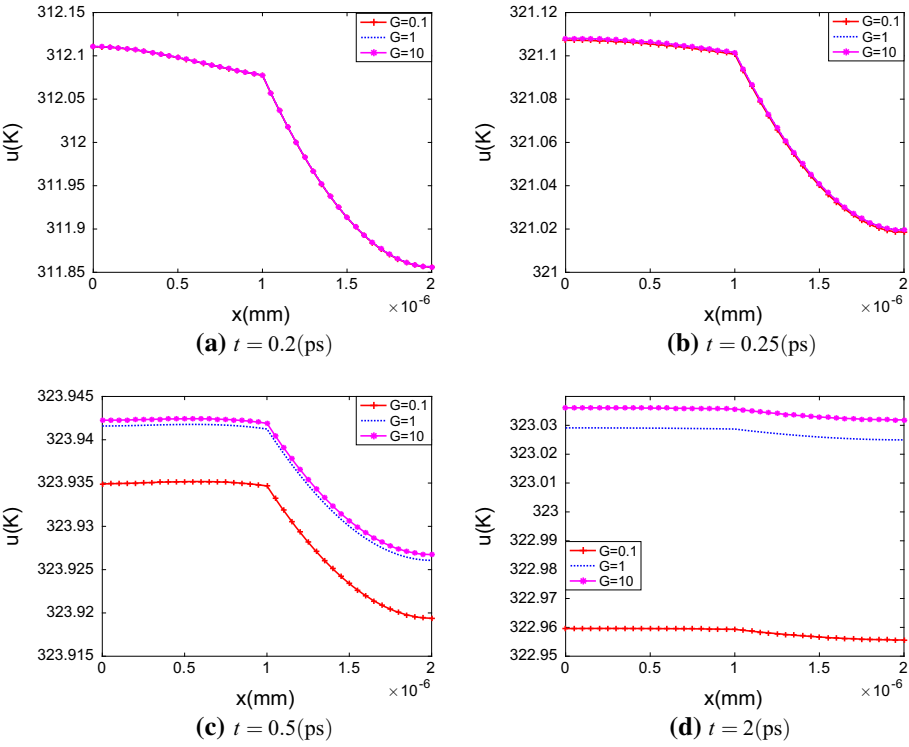

(a) $t = 0.2(\text{ps})$ **(b)** $t = 0.25(\text{ps})$

(c) $t = 0.5(\text{ps})$ **(d)** $t = 2(\text{ps})$

Fig. 7 Temperature profiles at $t = 0.2$ (ps), 0.25 (ps), 0.5 (ps), 2 (ps) for $(\alpha, \beta) = (0.9, 0.5)$

where c_4 is a positive constant independent of τ, h_1 and h_2.

From the Gronwall inequality, the conclusion holds. □

6 Numerical Experiments

In this section, we carry out some numerical experiments to study the performance and the convergence accuracy of the present numerical scheme. Then, we illustrate the applicability of the model (10)–(16) by predicting the temperature in a double-layered nanoscale thin film, where a gold layer is on a chromium padding layer exposed to an ultrashort-pulsed laser heating. All numerical computations were carried out by using MATLAB. And we exploit the Thomas algorithm to obtain the numerical results.

For simplicity, we set the space step sizes $h_1 = h_2 = h$. Since the analytical solution is not available for the general case, we use

$$\text{Error}_h(\tau) = \max_{0\le i\le M} \left| u_i^N(h,\tau) - u_i^{2N}\left(h, \frac{\tau}{2}\right)\right|,$$

$$\text{Error}_\tau(h) = \max_{0\le i\le M} \left| u_i^N(h,\tau) - u_{2i}^{N}\left(\frac{h}{2}, \tau\right)\right|$$

to measure the numerical errors in time and in space, respectively, where $u_i^N(h,\tau)$ denotes the numerical solution at grids (x_i, t_N). The corresponding temporal and spatial convergence orders are defined by

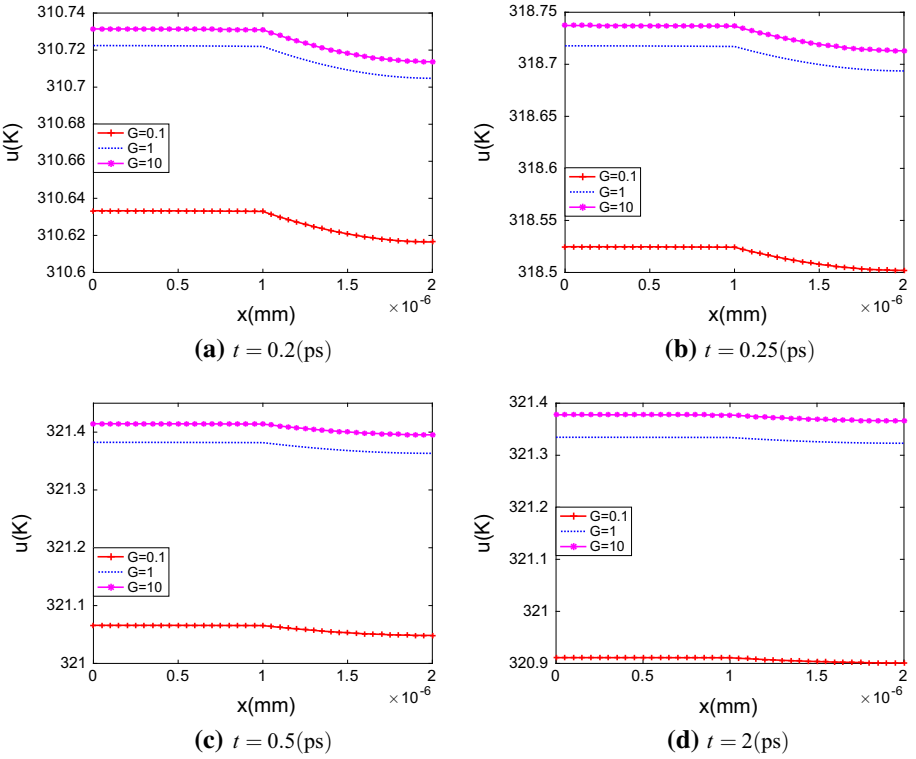

(a) $t = 0.2$(ps) **(b)** $t = 0.25$(ps)

(c) $t = 0.5$(ps) **(d)** $t = 2$(ps)

Fig. 8 Temperature profiles at $t = 0.2$ (ps), 0.25 (ps), 0.5 (ps), 2 (ps) for $(\alpha, \beta) = (0.1, 0.9)$

$$\mathrm{Order}_h(\tau) = \log_2 \frac{\mathrm{Error}_h(2\tau)}{\mathrm{Error}_h(\tau)}, \quad \mathrm{Order}_\tau(h) = \log_2 \frac{\mathrm{Error}_\tau(2h)}{\mathrm{Error}_\tau(h)}.$$

Example 1 Consider (10)–(16) with $\psi_1(x) = 0$, $\psi_2(x) = 0$, $\phi_1(t) = 0$, $\phi_2(t) = 0$, and the source term

$$\begin{cases} f_1(x,t) = \sin x, & 0 \le x \le 0.5, \\ f_2(x,t) = \cos x, & 0.5 \le x \le 1. \end{cases}$$

In this numerical experiment, the parameters are chosen as follows: $L_t = 1$, $l_x = 0.5$, $L_x = 1$, $B_1 = 1$, $B_2 = 1$, $\eta_1 = 1$, $\eta_2 = 1$, $\gamma_1 = 1$, $\gamma_2 = 1$.

We use the scheme (61)–(64) to obtain the numerical solution. Fixing $\tau = \frac{1}{500}$, Table 1 shows the numerical errors and the spatial convergence accuracy of the scheme for the Knudsen numbers $K_{\mathrm{n},1} = K_{\mathrm{n},2} = 0.1, 1, 10$, respectively. It should be pointed out that when the mean free path is constant, the larger the Knudsen number is, the smaller the characteristic length is. From Table 1, we see that the scheme achieves second-order convergence accuracy in space. Let $h = \frac{1}{100}$. Table 2 presents the corresponding numerical results in the temporal direction. As expected, our scheme gives the convergence accuracy of order $\min\{2-\alpha, 2-\beta\}$ in time.

Example 2 We considered the 1D time fractional DPL heat conduction equation in a double-layered nanoscale thin film where a gold layer is on a chromium padding layer exposed

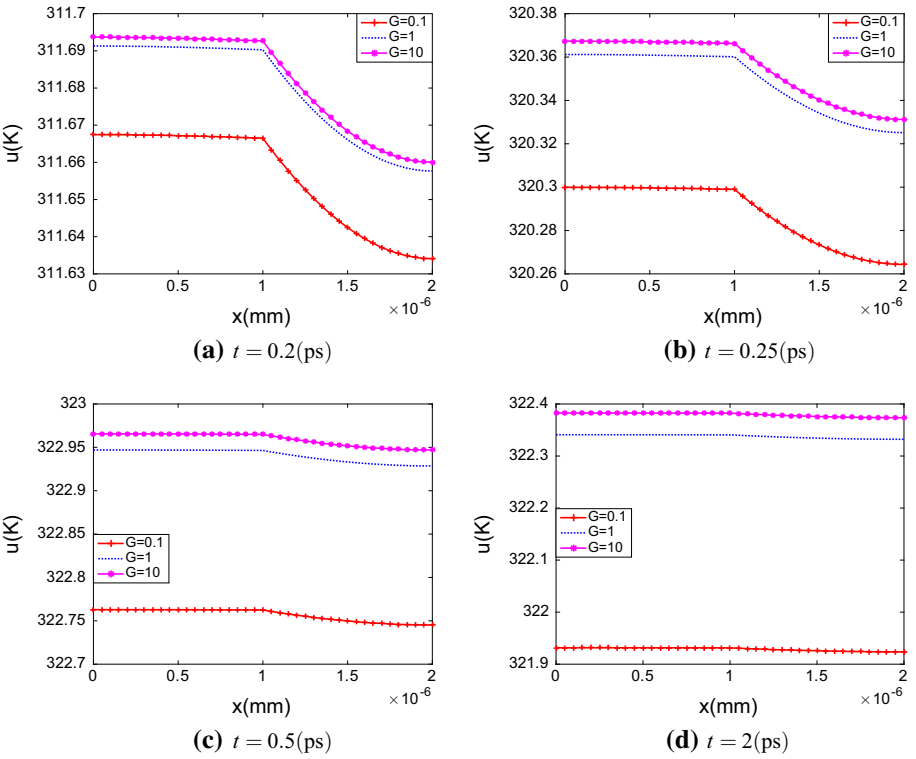

Fig. 9 Temperature profiles at $t = 0.2$ (ps), 0.25 (ps), 0.5 (ps), 2 (ps) for $(\alpha, \beta) = (0.5, 0.9)$

to an ultrashort-pulsed laser heating. Each thickness of the gold layer and the chromium layer is 1(nm), implying that $L_x = 2(\text{nm}), l_x = 1(\text{nm})$. The thermal properties of gold and chromium used in the analysis are listed in Table 3.

The heat source for both layers was given as

$$S(x,t) = 0.94J\frac{1-R}{t_p\delta}\exp\left[-\frac{x}{\delta} - 2.77\left(\frac{t-2t_p}{t_p^2}\right)^2\right]$$

where $J = 13.7(\text{J/m}^2)$, $\delta = 15.3(\text{nm})$, $t_p = 0.1(\text{ps})$ and $R = 0.93$. The initial temperature was chosen to be $T_0 = 300(\text{K})$. In this case, we chose $f_1(x,t) = S(x,t) + \frac{(\tau_{q,1})^\alpha}{\Gamma(1+\alpha)}\frac{C}{0}D_t^\alpha S(x,t)$ and $f_2(x,t) = S(x,t) + \frac{(\tau_{q,2})^\alpha}{\Gamma(1+\alpha)}\frac{C}{0}D_t^\alpha S(x,t)$ as given in (4). For simplicity, we fixed the following boundary conditions and initial conditions

$$\begin{aligned} -GT_x(0,t) + T(0,t) = T_0, \quad GT_x(L_x,t) + T(L_x,t) = T_0, \quad 0 < t < L_t, \\ T(x,0) = T_0, \quad T_t(x,0) = 0, \quad 0 \le x \le L_x. \end{aligned}$$

We used the scheme (61)–(64) to compute the numerical solution of this example. And here, we only considered the parameters $(\alpha, \beta) = (0.7, 0.3)$ and the computational accuracy at time $L_t = 1$ to check the convergence orders. We fixed the number of subintervals $N = 500$ and varied the space step size h to test the convergence order in space. On the other hand, in

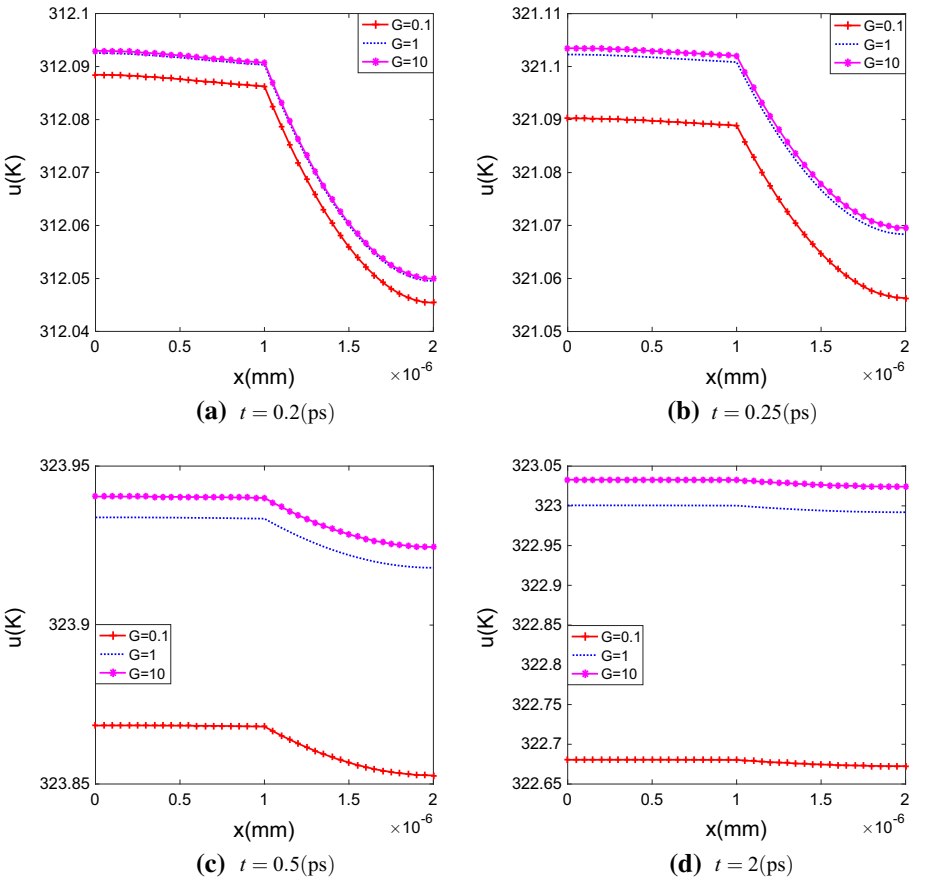

Fig. 10 Temperature profiles at $t = 0.2$ (ps), 0.25 (ps), 0.5 (ps), 2 (ps) for $(\alpha, \beta) = (0.9, 0.9)$

order to verify the convergence order in time, we used an adequately small space step size $h = \frac{1}{200}$ with different time step sizes. The numerical results in Table 4 and Table 5 indicate that the scheme (61)–(64) guarantees second-order accuracy in space and $\min\{2-\alpha, 2-\beta\}$ order accuracy in time which coincide with the theoretical results in Theorem 3.

Figures 2, 3, 4, 5, 6, 7, 8, 9 and 10 show the temperature profiles along the spatial direction for $G = 0.1, 1, 10$, at $t = 0.2$ (ps), 0.25 (ps), 0.5 (ps), 2(ps), respectively, with various pair (α, β). Numerical results were computed by using the time increment 0.025 (ps) and 40 grid points in space. From those figures, one can distinguish the temperature difference at the interface between these two layers at the beginning since thermal properties of gold and chromium are different. At $t = 2(ps)$, the temperature reaches the steady-state due to the nanoscale thickness. Furthermore, we see that the temperature level for $G = 10$ is highest, the temperature level for $G = 1.0$ is next, and the lowest one is for $G = 0.1$. This is because when G is larger, the boundary condition tends to be insulated, on the other hand, when G is smaller, the boundary condition tends to be the Dirichlet boundary condition. Fixing the fractional order $\beta = 0.1$ and varying $\alpha = 0.1, 0.5, 0.9$, we see that the temperature level heightens slightly as α increases. Similar results can be seen for $\beta = 0.5, 0.9$ cases.

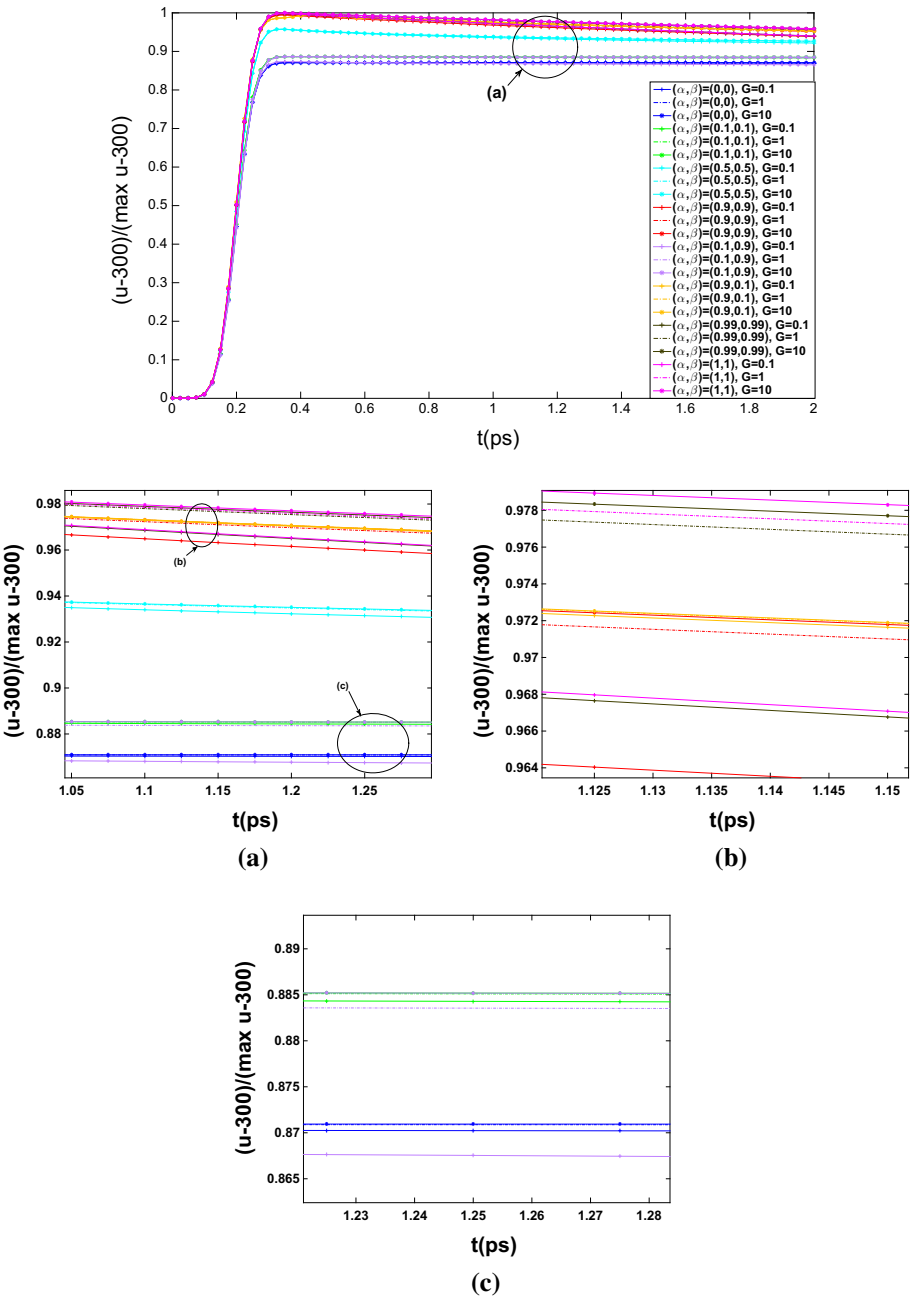

Fig. 11 Temperature profiles at $x = 0$ (nm) for different parameters (α, β) and G

Based on the same mesh girds of the above figures, Fig. 11 shows the temperature profiles along the temporal direction for all $(\alpha, \beta) = (0, 0)$, $(0.1, 0.1)$, $(0.5, 0.5)$, $(0.9, 0.9)$, $(0.1, 0.9)$, $(0.9, 0.1)$, $(0.99, 0.99)$, $(1, 1)$ and $G = 0.1, 1, 10$ at $x = 0$(nm). From this figure,

we see that the temperature changes from the traditional heat conduction equation to the DPL heat conduction equation with integer order derivatives. This vividly explains that the new model (10)–(16) may be used for modeling some type of sub-DPL heat conduction behavior. In addition, from Fig. 11, one may see that the temperature rises and reaches quickly the steady-state within $0 \leq t \leq 0.3$(ps), because of the very thin film. The maximum temperature is round about 324(K) when $\alpha = \beta = 0.99$ and $G = 10$, which are close to the integer order derivatives and the insulated boundary condition. The maximum temperature is almost identical to that obtained in [2], where the DPL equation has not fractional order derivatives.

7 Conclusion

We have developed a well-posed time fractional dual-phase-lagging (DPL) heat conduction equation in a double-layered nanoscale thin film with the temperature-jump boundary condition. An accurate finite difference scheme has been presented for solving this model. Unconditional stability and convergence of the scheme are proved in the maximum norm. Numerical results support the theoretical analysis and show the applicability to the nanoscale heat transfer in a double-layered thin film. Further research will focus on the development of high order accurate numerical schemes for the fractional DPL model in a double layered thin film, where the challenge lies in the interface. As such, one may obtain a reasonably accurate solution using a relatively coarse mesh. This is particularly interesting for thermal analysis in nanoscale heat conduction.

References

1. Jamshidi, M., Ghazanfarian, J.: Dual-phase-lag analysis of CNT–MoS_2–ZrO_2–SiO_2–Si nano-transistor and arteriole in multi-layered skin. Appl. Math. Model. **60**, 490–507 (2018)
2. Sun, H., Sun, Z.Z., Dai, W.: A second-order finite difference scheme for solving the dual-phase-lagging equation in a double-layered nanoscale thin film. Numer. Methods Partial Differ. Equ. **33**, 142–173 (2017)
3. Tzou, D.Y.: Macro- To Microscale Heat Transfer: The Lagging Behavior, 2nd edn. Wiley, New York (2015)
4. Ghazanfarian, J., Shomali, Z., Abbassi, A.: Macro- to nanoscale heat and mass transfer: the lagging behavior. Int. J. Thermophys. **36**, 1416–1467 (2015)
5. Nasri, F., Aissa, MFBen, Belmabrouk, H.: Effect of second-order temperature jump in metal-oxide-semiconductor field effect transistor with dual-phase-lag model. Microelectron. J. **46**, 67–74 (2015)
6. Saghatchi, R., Ghazanfarian, J.: A novel SPH method for the solution of dual-phase-lag model with temperature-jump boundary condition in nanoscale. Appl. Math. Model. **39**, 1063–1073 (2015)
7. Shomali, Z., Abbassi, A.: Investigation of highly non-linear dual-phase-lag model in nanoscale solid argon with temperature-dependent properties. Int. J. Therm. Sci. **83**, 56–67 (2014)
8. Dai, W., Han, F., Sun, Z.Z.: Accurate numerical method for solving dual-phase-lagging equation with temperature jump boundary condition in nanoheat conduction. Int. J. Heat Mass Transf. **64**, 966–975 (2013)
9. Ghazanfarian, J., Shomali, Z.: Investigation of dual-phase-lag heat conduction model in a nanoscale metal-oxide-semiconductor field-effect transistor. Int. J. Heat Mass Transf. **55**, 6231–6237 (2012)
10. Awad, E.: On the generalized thermal lagging behavior. J. Therm. Stress. **35**, 193–325 (2012)
11. Sherief, H.H., EI-Sayed, A.M.A., EI-Latief, A.M.A.: Fractional order theory of thermoelasticity. Int. J. Solid Struct. **47**, 269–275 (2010)
12. Caputo, M.: Linear models of dissipation whose Q is almost frequency independent—II. Geophys. J. Int. **13**, 529–539 (1967)
13. Youssef, H.M.: Theory of fractional order generalized thermoelasticity. J. Heat Transf. **132**, 061301 (2010)
14. Povstenko, Y.Z.: Fractional heat conduction equation and associated thermal stress. J. Therm. Stress. **28**, 83–102 (2005)

15. Yu, Y.J., Tian, X.G., Lu, T.J.: Fractional order generalized electro-magneto-thermo-elasticity. Eur. J. Mech. A Solids **42**, 188–202 (2013)
16. Kim, P., Shi, L., Majumdar, A., McEuen, P.: Thermal transport measurements of individual multiwalled nanotubes. Phys. Rev. Lett. **87**, 215502 (2001)
17. Balandin, A.A.: Thermal properties of graphene and nanostructured carbon materials. Nat. Mater. **10**, 569–581 (2011)
18. Tzou, D.Y.: Nonlocal behavior in phonon transport. Int. J. Heat Mass Transf. **54**, 475–481 (2011)
19. Ji, C.C., Dai, W., Sun, Z.Z.: Numerical method for solving the time-fractional dual-phase-lagging heat conduction equation with the temperature-jump boundary condition. J. Sci. Comput. **75**, 1307–1336 (2018)
20. Podlubny, I.: Fractional Differential Equations. Academic Press, New York (1999)
21. Liao, M., Gan, Z.H.: New insight on negative bias temperature instability degradation with drain bias of 28 nm high-K metal gate p-MOSFET devices. Microelectron. Reliab. **54**, 2378–2382 (2014)
22. Ho, J.R., Kuo, C.P., Jiaung, W.S.: Study of heat transfer in multilayered structure within the framework of dual-phase-lag heat conduction model using lattice Boltzmann method. Int. J. Heat Mass Transf. **46**, 55–69 (2003)
23. Liu, K.C.: Analysis of dual-phase-lag thermal behaviour in layered films with temperature-dependent interface thermal resistance. J. Phys. D Appl. Phys. **38**, 3722–3732 (2005)
24. Shen, M., Keblinski, P.: Ballistic vs. diffusive heat transfer across nanoscopic films of layered crystals. J. Appl. Phys. **115**, 144310 (2014)
25. Pillers, M., Lieberman, M.: Rapid thermal processing of DNA origami on silicon creates embedded silicon carbide replicas. In: 13th Annual Conference on Foundations of Nanoscience, Snowbird, Utah, April 11–16 (2016)
26. Tsai, T.W., Lee, Y.M.: Analysis of microscale heat transfer and ultrafast thermoelasticity in a multi-layered metal film with nonlinear thermal boundary resistance. Int. J. Heat Mass Transf. **62**, 87–98 (2013)
27. Sadasivam, S., Waghmare, U.V., Fisher, T.S.: Electron–phonon coupling and thermal conductance at a metal-semiconductor interface: first-principles analysis. J. Appl. Phys. **117**, 134502 (2015)
28. Ghazanfarian, J., Abbassi, A.: Effect of boundary phonon scattering on dual-phase-lag model to simulate micro- and nano-scale heat conduction. Int. J. Heat Mass Transf. **52**, 3706–3711 (2009)
29. Alikhanov, A.A.: A priori estimates for solutions of boundary value problems for fractional-order equations. Differ. Equ. **46**, 660–666 (2010)
30. Sun, Z.Z., Wu, X.N.: A fully discrete difference scheme for a diffusion-wave system. Appl. Numer. Math. **56**, 193–209 (2006)
31. Sun, Z.Z.: The Method of Order Reduction and Its Application to the Numerical Solutions of Partial Differential Equations. Science Press, Beijing (2009)
32. Feng, L.B., Liu, F., Turner, I., Zheng, L.C.: Novel numerical analysis of multi-term time fractional viscoelastic non-Newtonian fluid models for simulating unsteady MHD Couette flow of a generalized Oldroyd-B fluid. Fract. Calc. Appl. Anal. **21**, 1073–1103 (2018)